Copy No. 15

DEFENCE R&D DÉFENSE

A FLAT-FACET QUADRILATERAL ELEMENT FOR LINEAR ELASTIC ANALYSIS OF LAMINATED COMPOSITE PLATES AND SHELLS

M.J. Smith

DEFENCE RESEARCH ESTABLISHMENT ATLANTIC

Technical Memorandum

DREA TM 1999-210

January 2000

National Defence Défense nationale

Canada

102-02563/

National Defence
Research and Development Branch

Défense nationale
Bureau de recherche et développement

A FLAT-FACET QUADRILATERAL ELEMENT FOR LINEAR ELASTIC ANALYSIS OF LAMINATED COMPOSITE PLATES AND SHELLS

Malcolm J. Smith

January 2000

Approved by J. L. Kennedy:
Head/ Warship Signatures and Safety

TECHNICAL MEMORANDUM 1999-210

Defence Research Establishment Atlantic

Centre de Recherches pour la Défense Atlantique

Canada

Abstract

A flat-facet quadrilateral shell element 'Shell4' has been developed for linear-elastic static finite element (FE) analysis of laminated composite and non-composite applications in ship structures. The element formulation was developed by combining state-of-the-art formulations for quadrilateral plate bending and quadrilateral membrane elements with first-order shear deformation theory (FSDT) for laminates. The element is intended for use with general plate and shell configurations, involving isotropic, orthotropic, or composite material properties. In-plane rotations, also known as drilling degrees of freedom, have been included to permit correct element assembly in kinked or folded-plate type configurations, and special provision has been made for warped geometries. The element has been implemented in a finite element programme recently developed at DREA for linear static and first-ply failure analysis of composite structures. It is shown to pass all of the necessary patch tests to guarantee convergence. Validation is carried out using examples of isotropic beam and shell structures and composite plates taken from the finite element literature. The element is found to perform excellently for a number of problems involving a simply supported, uniformly-loaded composite plate. In shell and beam applications its performance is acceptable, although the element appears slow to converge at locations where concentrated loads are applied or in situations where elements are warped. The membrane response alone, however, appears to be quite good, and the element is less affected by mesh distortions than some other commercially available elements.

Résumé

Un élément de coque quadrilatéral à face plate, « Shell 4 », a été mis au point pour l'analyse élastique linéaire statique par éléments finis des applications de matériaux composites et non composites stratifiés sur les structures de navires. La formulation de l'élément a été élaborée en combinant des formulations de pointe sur le cintrage des plaques quadrilatérales et des éléments de membrane quadrilatéraux avec la théorie de premier ordre du cisaillement des stratifiés. L'élément doit être utilisé pour les configurations générales de plaques et de coque ayant des propriétés de matériau isotropique, orthotropique ou composite. Des rotations dans le plan, aussi appelées degrés de liberté de perçage, ont été incluses pour permettre l'assemblage adéquat de l'élément dans des configurations de type faussées ou à plaque pliée, et des dispositions spéciales ont été prises pour les géométries faussées. L'élément a été mis en place dans un programme à éléments finis mis au point récemment au CRDA pour l'analyse linéaire statique et l'analyse des défaillances de l'épaisseur supérieure des structures composites. Il a réussi tous les essais à la pièce nécessaires pour garantir la convergence. La validation est effectuée à l'aide d'exemples de poutre et de structures de coque isotropiques et de plaques composites pris dans la documentation sur les éléments finis. L'élément fournit un excellent rendement pour plusieurs problèmes relatifs à une plaque composite à charge uniforme libre aux extrémités. Pour la coque et les poutres, son rendement est acceptable, même si l'élément semble lent à converger aux emplacements où des charges concentrées sont appliquées ou dans les situations où des éléments sont faussés. La réponse de membrane seule, cependant, semble être assez bonne et l'élément est moins touché par les distorsions de maille que d'autres éléments disponibles dans le commerce.

Contents

Abstract i

Résumé i

List of Figures iv

List of Tables v

Executive Summary vi

1 Introduction 1

2 First-Order Shear Deformation Theory 3
2.1 Layer Mechanics 4
2.2 Laminate Mechanics 5

3 Isoparametric Shape Functions 8

4 Drilling Degrees of Freedom 11

5 Improving In-Plane Behaviour With Internal Shapes 12

6 Mixed Interpolation of Transverse Shear 13

7 Element Stiffness Formulation 14
7.1 Flat Element Stiffness Matrix 14
7.2 Numerical Integration 16
7.3 Removal of Rigid Body Mechanism in Drilling DOF [15] 17
7.4 Correction for Warping 17

8 Implementation and Solution 19

9 Post-Computation of Stresses 20

10 Numerical Validation 21
10.1 Patch Tests 21
10.2 Obstacle Course Example Problems 23
10.2.1 Cantilevered Beam 23
10.2.2 Twisted Beam 25
10.2.3 Scordelis-Lo Roof 25
10.2.4 Pinched Cylinder 27
10.2.5 Hemispherical Shell 27
10.3 Composite Plate Examples 29

10.3.1 Thin Plate Under Uniform Loading 29
10.3.2 Effect of Plate Thickness 30

11 Conclusions 33

Acknowledgements 33

References 33

List of Figures

1 Typical FRP layer with unidirectional fibres showing the fibre-matrix coordinate system. 5
2 Coordinates defining layer positions within a laminate. 7
3 Geometric configuration and local frame of reference. 9
4 Natural coordinate system. 10
5 Mid-side points used to interpolate the transverse shear deformation. 13
6 Characterization of warping as a distance H from an unwarped middle plane. 18
7 Five patch tests used to verify convergence of a four-node shell element [29]. 22
8 Five element mesh used for all patch tests. 23
9 Regular and distorted meshes for a cantilevered beam (not to scale). 25
10 Twisted cantilever beam with a 4×2 mesh. 26
11 Scordelis-Lo roof problem showing a 2×2 meshed region. 26
12 One-eighth model of a cylindrical shell with a 2×2 mesh. 27
13 One-quarter model of a hemispherical shell with a 4×4 mesh. 28
14 Modelled region for simply supported plates. 29

List of Tables

1 Patch test results. 21
2 Finite element results for the obstacle course example problems (displacements expressed as a ratio of the theoretical values). 24
3 Boundary conditions for enforcing symmetry. 30
4 Results for four simply supported plate models. 31
5 Normalized quantities and their evaluation points for thin plate results (G.P. = Gauss point). 31
6 Effect of thickness changes in a simply-supported, three-layer composite plate. 32
7 Normalized quantities and their evaluation points for thick plate results (G.P. = Gauss point). 32

DREA TM 1999-210

A Flat-Facet Quadrilateral Element for Linear Elastic Analysis of Laminated Composite Plates and Shells

by
Malcolm J. Smith

Executive Summary

Background

Fibre-reinforced polymers (FRPs) are finding increased application in naval structures and platforms, due primarily to their superior strength-to-weight ratio and resistance to corrosion. In particular, the anticipated application of FRP composities in a new lightweight mast for the Halifax class frigate has spurred interest in acquiring in-house capabilities in composite materials at DREA, especially in the areas of finite element modelling and analysis. To some extent, this type of work can be performed with existing commercial codes; however, limitations in the material modelling capabilities and in the availability of good general-purpose composite elements, make some level of in-house finite element (FE) development advisable.

Current meshing practices for ship structures at DREA call for four-node quadrilateral shell elements. Both the MGDSA (Maestro Graphics Detailed Stress Analysis) software and the recently developed Detail Analysis of Ship Structures (DASS) methodology predominantly rely on this element. If finite element analysis of composites is to be compatible with these tools, a four-node quadrilateral composite shell will be required. The ANSYS finite element programme, now being used at DREA, has two eight-node composite shell elements, one for linear analysis and one for nonlinear analysis. DREA's VAST finite element programme currently has two eight-node composite shell elements, both for linear analysis, but both of which use special material models to account for through-thickness effects. The additional degrees of freedom and computational load required by these elements makes them unsuitable for general purpose use.

Principal Results

A flat-facet quadrilateral shell element 'Shell4' has been developed for linear-elastic static analysis of laminated composite and non-composite applications in ship structures. The element formulation was developed by combining state-of-the-art formulations for quadrilateral plate bending and quadrilateral membrane elements with first-order shear deformation theory (FSDT) for laminates. The Shell4 element has been implemented in a new finite element programme, FELAM, recently developed at DREA for linear static and first-ply failure analysis of composite plates and shells. It is shown to pass all of the necessary patch tests

to guarantee convergence. Validation is carried out using examples of isotropic beam and shell structures and composite plates taken from the finite element literature. No evidence of transverse shear locking or spurious modes has been observed in any of the examples tested to date. The element is found to perform excellently in composite plate examples when compared to an ANSYS quadratic element. In shell and beam applications its performance is acceptable, but it exhibits slow convergence in some situations. The performance of the element degrades sharply when it is in a warped configuration, but is less sensitive than other elements to shape distortion in its membrane response.

Significance of Results

The element developed in this study is based on a material model sufficiently general that it can be used with most FRP solid laminate, sandwich composite, and metallic materials, all of which are important in marine applications. Layers within laminates may be either isotropic or orthotropic, thereby allowing for unidirectional, woven-roving, or chopped-strand fibres. In the current version of FELAM, the element is limited to linear-elastic static and first-ply failure analysis, of which only the former is discussed in this Memorandum. In addition, the implementation is limited to relatively small problems due to an inefficient equation solution algorithm currently being used in FELAM. This prevents the element from being tested on more realistic ship-structure problems, and to date the largest structure that has been successfully solved had a size of 256 nodes (1536 degress of freedom). Accuracy tests performed on small beam, plate, and shell problems have verified that the element does converge to theoretical solutions as meshes are refined, thereby confirming the results of five patch tests.

Future Work

Future capabilities that will be needed for the Shell4 element include dynamic/modal analysis, linear buckling and nonlinear failure analysis. Although the development to this stage has been generally successfully, the author considers it advisable to conduct further research on element formulations before extending the Shell4 element to other analysis types. Of particular importance is assessing the element formulation's suitability for use in nonlinear failure analysis, which is important in determining the ultimate strength of ship sections and components. Also, the current linear-elastic implementation of the element will be tested on more realistic ship-structure problems once an efficient equation solver becomes available.

1 Introduction

Fibre-reinforced polymers (FRPs) are finding increased application in naval structures and platforms, due to their superior strength-to-weight ratio and resistance to corrosion. In particular, the anticipated application of FRP composities in the Halifax class frigate has spurred interest in acquiring in-house capabilities in composite materials at DREA, especially in the area of finite element analysis. To some extent, this type of work can be performed with commercial codes such as ANSYS [1]. Limitations in existing codes, especially in material modelling and the variety of composite-capable elements, make some level of in-house finite element (FE) development desirable, either within DND's VAST programme [2] or within another application. In-house development would have the added advantage of easier integration with existing DND codes for database management, meshing, and visualization.

Of particular interest is the formulation of an element for general-purpose use in ship structure applications. Traditionally, the most useful element for metallic ship structures has been the flat-facet quadrilateral shell, for reasons of its wide applicability, low computational cost, and ease of meshing. Current meshing practices for ship structures at DREA call for four-node quadrilateral shell elements. Both the MGDSA (Maestro Graphics Detailed Stress Analysis) software [3] and the recently developed Detail Analysis of Ship Structures (DASS) [4] methodology predominantly rely on this element. If finite element analysis of composites is to be compatible with these tools, a four-node quadrilateral composite shell will be required. The ANSYS finite element programme, now being used at DREA, has two eight-node composite shell elements, one for linear analysis and one for nonlinear analysis. In lieu of a four node element, these two elements appear to be suitable for general purpose use. DREA's VAST finite element programme currently has two eight-node composite shell elements, both for linear analysis, but both of which use special material models to account for through-thickness effects. One element is based on a refined (i.e., higher-order approximation of transverse shear) theory and the other is based on a multilayer theory. The additional degrees of freedom and computational load required by these elements makes them unsuitable for general purpose use.

The aim of the present study is to develop a flat-facet quadrilateral element that can be used for FRP laminate and FRP laminate-core sandwich construction, as well as for conventional isotropic materials. Provided satisfactory performance can be obtained, this element could eventually supercede the existing quadrilateral shell element in VAST, and find widespread application in the analysis of both composite or metallic ship structures. At present, however, the element is being developed for linear static analysis only, with future application to vibration, buckling, and nonlinear post-failure analysis being considered.

Composite shell elements have evolved as either adaptations of existing, isotropic elements, or as entirely new element types derived for a particular composite material model. The latter group is more apparent in the published literature, no doubt due to the uniqueness of the formulations. However, their dependence on a particular composite material model inevitably makes them less suitable for general purpose applications. For the purposes of the present study, the ideal composite shell element would be based on a generalised mate-

rial model, which could then be adapted to a particular material type (e.g., FRP laminate, sandwich, steel) or configuration, composite or otherwise.

For this reason the approach taken in this study was to develop a new composite shell element from a class of elements proven to be effective with isotropic materials. Being able to apply a single element type for both composite and non-composite materials provides many advantages, including reduced development and maintenance of coding and simplified meshing requirements.

Existing isotropic shell elements fall into a number of general classes, among which the most significant are (1) flat-facet shells developed by combining plate and membrane formulations; (2) degenerate-solid shells developed from three-dimensional solid formulations; and (3) hybrid formulations using a mixture of displacement-based and stress- or strain-based interpolation functions. The flat-facet shell approach, which is described in a number of finite element textbooks [5, 6], produces formulations that are relatively versatile and computationally simple. The hybrid approach, on the other hand, produces the most computationally intensive formulations. Moreover, the hybrid approach employing stress-based interpolation functions, while effective for isotropic materials, would be inappropriate for composite elements because of the very complicated stress fields that occur in a laminate. Hybrid formulations for composite elements have been developed using strain-based interpolation functions [7, 8]. The degenerate solid approach is the most advantageous where curved geometries or non-uniform thickness are being modelled. In linear analysis of ship structures, hulls, decks, and superstructures are adequately represented as connected flat surfaces, and curved geometry capabilities are generally not required. In an analysis with geometric nonlinearities the ability to model structures deformed with finite curvature is more important, and degenerate shell formulations have found favour in this area [9, 10]. Plating of non-uniform thickness is seldom encountered in ship structures, except in the modeling of unevenly corroded plates. The degenerate shell approach has typically been used with eight- or nine-node quadratic elements [11, 12], although successful four-node elements have also been developed [13, 14].

Based on these considerations, the flat-facet approach was chosen. A four-node quadrilateral configuration was preferred, since quadrilateral shells are known to be more accurate than triangular shells, and fit well with existing meshing algorithms. The element formulation presented here is developed along the lines of the isotropic quadrilateral shell proposed by Cook [15]. An isoparametric formulation of the membrane behaviour, supplemented by in-plane, or "drilling" rotations, is used in a manner similar to the membrane element proposed by MacNeal and Harder [16]. The membrane response is also supplemented with internal "bubble" functions, which are subsequently statically condensed from the element stiffness. Out-of-plane behaviour is based on the isoparametric formulation of plate bending, with mixed interpolation of transverse shear. This approach is used with Mindlin plate theory in the isotropic elements developed by Hughes and Tezduyar [17] and Bathe and Dvorkin [14, 18, 19]. It gives a more satisfactory solution to the problem of shear locking in thin elements, as opposed to the selectively-reduced integration approach used by Taylor et al. [20]. In the element formulation presented here, Mindlin plate theory is replaced by First-Order

Shear Deformation Theory (FSDT) for composite laminates. FSDT is discussed in detail in Section 2. The laminate arrangement is in general non-symmetric, therefore allowing for coupling between membrane and bending deformations. Each ply may have isotropic or orthotropic properties, making it possible to represent most types of FRP laminates with unidirectional, woven-roving, or chopped-strand plies. Sandwich composites consisting of a lightweight core material layer between two laminated face plates can also be modelled. Metal plating can be treated as a single-layer laminate of isotropic material.

To simplify the presentation, only linear-elastic static analysis is considered in this study. Once the element has been fully validated for a range of linear static problems, application to other analysis types will be considered. The element formulation has been derived with future applications in mind, and extension to nonlinear static, buckling, vibration, first-ply failure and post-failure analysis should be possible. The element has been implemented in an object-oriented finite element code FELAM, developed recently at DREA. At present the code is only equipped with an in-core dense matrix solver, and is therefore only practically applicable to meshes with less than 500 nodes. Several examples are given in Section 10 for validation purposes. In these examples, both composite and isotropic materials are used and comparisons are made with ANSYS, VAST and analytical results, where available.

2 First-Order Shear Deformation Theory

Theories describing the mechanics of composite laminates fall into three general categories: equivalent single-layer theories, higher-order or "refined" theories, and multi-layer theories. From a finite element standpoint, equivalent single-layer theories are the easiest to work with. The properties of multiple-layer laminates are combined together into a simple set of linear equations that can, with a little additional work, be employed directly in finite element formulations for shells that were originally developed for isotropic or anisotropic materials. Equivalent single-layer theories have been developed based on Kirchoff-like assumptions (Classical Laminate Theory) and Mindlin-like assumptions about shear deformation (First-Order Shear Deformation Theory).

Higher-order theories [21, 22] try to improve the representation of shear deformation by including higher than linear terms in the through-thickness direction of the displacement field. Finite elements based on these theories have more than the standard number of nodal degrees of freedom (DOFs) used in equivalent single-layer elements [23, 24]. This naturally leads to greater computational expense, as well as uncertainty over what boundary conditions should be applied to the additional DOFs. Similarly, multi-layer theories [25] produce a more accurate representation of shear deformation and other through-thickness effects by modelling each layer of the laminate separately. This leads to finite elements with two or more extra DOFs per node for each extra layer. In the majority of applications, the extra accuracy obtained with higher-order or multilayered theories is not significant enough to justify the additional expense. Therefore they are not recommended for general purpose use, but rather for special applications where interlaminar shear and other through-thickness effects are of particular interest.

In many fibre-reinforced polymer materials the ratio of the shear modulus to the elastic modulus in the fibre direction is much smaller than occurs in isotropic materials. Laminates of these materials are therefore susceptible to thickness effects at smaller thickness-to-side-length ratios, making the inclusion of some measure of shear deformation important. For this reason, First-Order Shear Deformation Theory (FSDT), as described by Reddy [26], was chosen as the material model for the shell element developed in this study.

2.1 Layer Mechanics

A typical orthotropic layer is defined with reference to a ply with unidirectional fibres (see Figure 1). A fibre-matrix coordinate system 123 is defined, in which 1 is in the direction of the fibres, 2 is perpendicular to the fibres in the plane of the layer, and 3 is perpendicular to the layer. Using plane stress assumptions for the layer, a linear stress-strain relationship can be defined in terms of the basic material properties. These include the two in-plane elastic moduli E_1 and E_2, the shear moduli in three orthogonal planes G_{12}, G_{13}, G_{23}, and the Poisson's ratio ν_{12}. Assuming the normal stress in the 3 direction to be zero, the stress-strain relation is written as [26]

$$\begin{Bmatrix} \sigma_1 \\ \sigma_2 \\ \tau_{12} \\ \tau_{13} \\ \tau_{23} \end{Bmatrix} = \begin{bmatrix} C_{11} & C_{12} & 0 & 0 & 0 \\ C_{12} & C_{22} & 0 & 0 & 0 \\ 0 & 0 & C_{33} & 0 & 0 \\ 0 & 0 & 0 & C_{44} & 0 \\ 0 & 0 & 0 & 0 & C_{55} \end{bmatrix} \begin{Bmatrix} \epsilon_1 \\ \epsilon_2 \\ \gamma_{12} \\ \gamma_{13} \\ \gamma_{23} \end{Bmatrix} \tag{1}$$

or

$$\overline{\sigma} = \mathbf{C}\overline{\epsilon} \tag{2}$$

where $\overline{\sigma} = \{\sigma_1\ \sigma_2\ \tau_{12}\ \tau_{13}\ \tau_{23}\}^T$ is the stress vector, $\overline{\epsilon} = \{\epsilon_1\ \epsilon_2\ \gamma_{12}\ \gamma_{13}\ \gamma_{23}\}^T$ is the strain vector, and where C_{ij} are elastic constants of the layer in the 123 coordinate system. These are related to the material properties as follows

$$\begin{aligned} C_{11} &= \frac{E_1}{1-\nu_{12}\nu_{21}} \quad C_{12} = \frac{\nu_{12}E_2}{1-\nu_{12}\nu_{21}} \quad C_{22} = \frac{E_2}{1-\nu_{12}\nu_{21}} \\ C_{33} &= G_{12} \qquad C_{44} = G_{13} \qquad C_{55} = G_{23} \qquad \frac{\nu_{12}}{E_1} = \frac{\nu_{21}}{E_2} \end{aligned} \tag{3}$$

The same stress-strain relation can be written for a rotated coordinate system xyz in which z is perpendicular to the plane of the layer:

$$\sigma = \mathbf{Q}\epsilon \tag{4}$$

where $\sigma = \{\sigma_x\ \sigma_y\ \tau_{xy}\ \tau_{xz}\ \tau_{yz}\}^T$ and $\epsilon = \{\epsilon_x\ \epsilon_y\ \gamma_{xy}\ \gamma_{xz}\ \gamma_{yz}\}^T$. Assuming that the 1 axis makes an angle θ to the x axis, the stiffness matrix $\mathbf{Q}$ is obtained as

$$\mathbf{Q} = \mathbf{T}^T\mathbf{C}\mathbf{T} \tag{5}$$

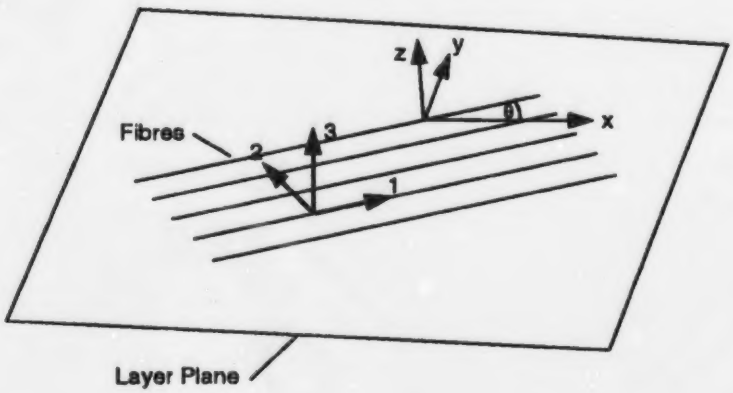

Figure 1: Typical FRP layer with unidirectional fibres showing the fibre-matrix coordinate system.

where

$$\mathbf{T} = \begin{bmatrix} c^2 & s^2 & cs & 0 & 0 \\ s^2 & c^2 & -sc & 0 & 0 \\ -2cs & 2sc & (c^2 - s^2) & 0 & 0 \\ 0 & 0 & 0 & c & s \\ 0 & 0 & 0 & -s & c \end{bmatrix} \tag{6}$$

with $c = \cos\theta$ and $s = \sin\theta$.

2.2 Laminate Mechanics

A laminate is made up of one or more layers rigidly bonded together in which the fibre axis of each layer may have a different orientation. First-order shear deformation theory (FSDT) is an equivalent single-layer theory, i.e., it describes the overall mechanical properties of the laminate as though it were a single unit. In this approach, the displacement of the cross-section as a whole is described with a single-set of equations:

$$\begin{aligned} u(x,y,z) &= u_0(x,y) + z\theta_y(x,y) \\ v(x,y,z) &= v_0(x,y) - z\theta_x(x,y) \\ w(x,y,z) &= w_0(x,y) \end{aligned} \tag{7}$$

Here u, v, and w are the displacements in the x, y, and z directions respectively. u_0, v_0, and w_0 are the displacements at the mid-plane, and θ_x and θ_y are rotations about the x and y axes, respectively.

Linear strain assumptions are used in which the strain in the plane of the laminate is given by,

$$\epsilon = \epsilon^{(0)} + z\epsilon^{(1)} \tag{8}$$

where

$$\epsilon^{(0)} = \left\{ \begin{array}{c} \epsilon^{(0)}_{xx} \\ \epsilon^{(0)}_{yy} \\ \gamma^{(0)}_{xy} \end{array} \right\} = \left\{ \begin{array}{c} u_{0,x} \\ v_{0,y} \\ u_{0,y} + v_{0,x} \end{array} \right\} \qquad \epsilon^{(1)} = \left\{ \begin{array}{c} \epsilon^{(1)}_{xx} \\ \epsilon^{(1)}_{yy} \\ \gamma^{(1)}_{xy} \end{array} \right\} = \left\{ \begin{array}{c} \theta_{x,x} \\ -\theta_{y,y} \\ \theta_{x,y} - \theta_{y,x} \end{array} \right\} \tag{9}$$

In this notation, $\epsilon^{(0)}$ is the in-plane strain at the mid-plane and $\epsilon^{(1)}$ is the curvature of the mid-plane. Comma notation has been used to denote partial differentation. Additional strain expressions are required for the out-of-plane shear deformation, given as

$$\gamma = \left\{ \begin{array}{c} \gamma_{xz} \\ \gamma_{yz} \end{array} \right\} = \left\{ \begin{array}{c} w_{,x} + \theta_y \\ w_{,y} - \theta_x \end{array} \right\} \tag{10}$$

The equilibrium equations are developed in stress resultant form by considering the balance of forces and moments on an infinitesimal area of laminate. Neglecting body moments and surface shearing forces, the static equations of motion in the presence of applied transverse forces q is given by:

$$\begin{aligned} N_{xx,x} + N_{xy,y} &= 0 \\ N_{xy,x} + N_{yy,y} &= 0 \\ Q_{x,x} + Q_{y,y} &= q(x,y) \\ M_{xx,x} + M_{xy,y} &= Q_x \\ M_{xy,x} + M_{yy,y} &= Q_y \end{aligned} \tag{11}$$

where N_{xx}, N_{yy} and N_{xy} are the in-plane force resultants, Q_x and Q_y are the out-of-plane force resultants, and M_{xx}, M_{yy} and M_{xy} are the out-of-plane moment resultants.

Alternatively, equilibrium within an element can be represented in the following variational form:

$$\begin{aligned} 0 = \int_{\Omega^e} \Bigg[& \left\{ \begin{array}{ccc} \delta\epsilon^{(0)}_{xx} & \delta\epsilon^{(0)}_{yy} & \delta\gamma^{(0)}_{xy} \end{array} \right\} \left\{ \begin{array}{c} N_{xx} \\ N_{yy} \\ N_{xy} \end{array} \right\} + \left\{ \begin{array}{ccc} \delta\epsilon^{(1)}_{xx} & \delta\epsilon^{(1)}_{yy} & \delta\gamma^{(1)}_{xy} \end{array} \right\} \left\{ \begin{array}{c} M_{xx} \\ M_{yy} \\ M_{xy} \end{array} \right\} \\ & + \left\{ \begin{array}{cc} \delta\gamma_{xz} & \delta\gamma_{yz} \end{array} \right\} \left\{ \begin{array}{c} Q_x \\ Q_y \end{array} \right\} - q\delta w \Bigg] \, dx \, dy \end{aligned} \tag{12}$$

or more compactly as,

$$0 = \int_{\Omega^e} \left[\{\delta\epsilon^{(0)}\}^T \{N\} + \{\delta\epsilon^{(1)}\}^T \{M\} + \{\delta\gamma\}^T \{Q\} - q\delta w \right] dx \, dy \tag{13}$$

where $N = \{N_{xx} \; N_{yy} \; N_{xy}\}^T$, $M = \{M_{xx} \; M_{yy} \; M_{xy}\}^T$, and $Q = \{Q_x \; Q_y\}^T$. The δ quantities are virtual strains, and the integration is performed over the element area Ω^e. By the principle of virtual work, the integral must be zero when the element is in equilibrium provided the virtual strains are admissible.

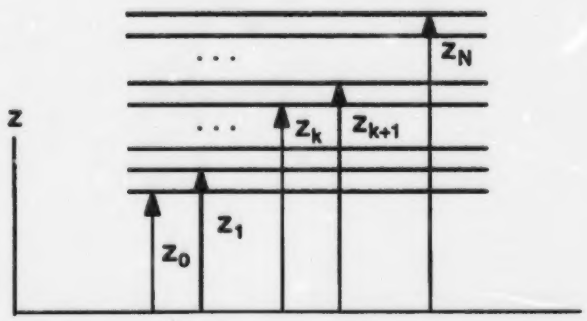

Figure 2: Coordinates defining layer positions within a laminate.

The relationship between the stress resultants and the strains is obtained by integrating the stress-strain equations for each layer throughout the entire thickness of the laminate. The resulting relations are expressed succinctly as [26]

$$\left\{ \begin{array}{c} N \\ M \end{array} \right\} = \left[\begin{array}{cc} A & B \\ B & D \end{array} \right] \left\{ \begin{array}{c} \epsilon^{(0)} \\ \epsilon^{(1)} \end{array} \right\} \tag{14}$$

$$\{Q\} = [E]\,\{\gamma\} \tag{15}$$

The elements of the matrices A, B, D, and E are obtained by the following integrals:

$$\begin{aligned} (A_{ij}, B_{ij}, D_{ij}) &= \sum_k \int_{z_k}^{z_{k+1}} Q_{ij}^{(k)}(1, z, z^2)\,\mathrm{d}z \qquad i,j = 1\ldots3 \\ E_{ij} &= \sum_k \int_{z_k}^{z_{k+1}} \kappa_i \kappa_j Q_{ij}^{(k)}\,\mathrm{d}z \qquad i,j = 4,5 \end{aligned} \tag{16}$$

where $Q_{ij}^{(k)}$ is the (i,j) element of the kth layer's stiffness given in Equation (5). The through-thickness positions z_k and z_{k+1} are shown Figure 2.

In Eq. (16), the coefficients κ_i are shear correction factors to compensate for through-thickness variations in the transverse shear stress. For isotropic materials, the distribution is parabolic so that $\kappa_i^2 = 5/6$. For laminates of fibre-reinforced layers, determining shear correction factors is more complicated, as the stress distribution through the thickness is highly dependent on the fibre orientation in each layer. The procedure used in this study is adapted from the one developed by Whitney [27]. In this approach cylindrical bending is assumed in each of the coordinate directions, and the exact transverse shear stress is calculated in each layer of the laminate. Then, by equating the exact shear strain energy with that predicted with the equivalent single-layer theory, the necessary correction factors are computed directly.

Considering cylindrical bending about the y-axis of a laminate. Whitney and Pagano [28] show that the x component of the stress field in the kth layer is given by

$$\sigma_{xx,x}^{(k)} = \frac{Q_{11}^{(k)}}{\Delta}(-B_{11} + zA_{11})Q_x \tag{17}$$

where $\Delta = A_{11}D_{11} - B_{11}^2$ and Q_x is the shear resultant. The transverse shear stress in the kth layer can then be obtained from stress equilibrium considerations as

$$\tau_{xz}^{(k)} = \int \sigma_{xx,x}^{(k)}\,\mathrm{d}z = -\frac{Q_{11}^{(k)}}{\Delta}(zB_{11} - \frac{z^2}{2}A_{11})Q_x + a^{(k)} \tag{18}$$

where $a^{(k)}$ is an integration constant. The first integration constant $a^{(0)}$ can be obtained by using the traction-free condition on the bottom surface of the laminate. The remainder can then be calculated by satisfying shear stress equilibrium at the layer interfaces.

The shear strain energy density $g^k(z)$ in each layer is determined from

$$g^k(z) = S_{xz}^{(k)}\left(\tau_{xz}^{(k)}\right)^2 = S_{xz}^{(k)}\left(a^{(k)} - \frac{Q_{11}^{(k)}}{\Delta}(zB_{11} - \frac{z^2}{2}A_{11})\right)^2 Q_x^2 \tag{19}$$

Integrating this over z gives the total shear strain energy in the laminate, V_s, which is then equated with the equivalent single-layer result of $E_{44}Q_x^2 = \kappa_1^2 A_{44}Q_x^2$. Hence the following expression is obtained for the shear correction factor:

$$\kappa_1^2 = \left[A_{44}\int_{-h/2}^{h/2} g^m(z)\,\mathrm{d}z\right]^{-1} \tag{20}$$

Assuming cylindrical bending about the x-axis, κ_2 can be determined in a similar manner.

3 Isoparametric Shape Functions

The four-node quadrilateral element developed here is depicted in Figure 3. A local coordinate system xyz is shown based on the nodal positions and which in general may be different from the laminate coordinate system referenced in the previous section, although a different notation is not necessary. The position of a point on the nodal plane of the element can be described in terms of the nodal positions and appropriate shape functions extending over the domain of the element. This can be written as

$$\begin{aligned} x &= \sum_{i=1}^{4} \psi_i(\xi,\eta)x_i^e \\ y &= \sum_{i=1}^{4} \psi_i(\xi,\eta)y_i^e \end{aligned} \tag{21}$$

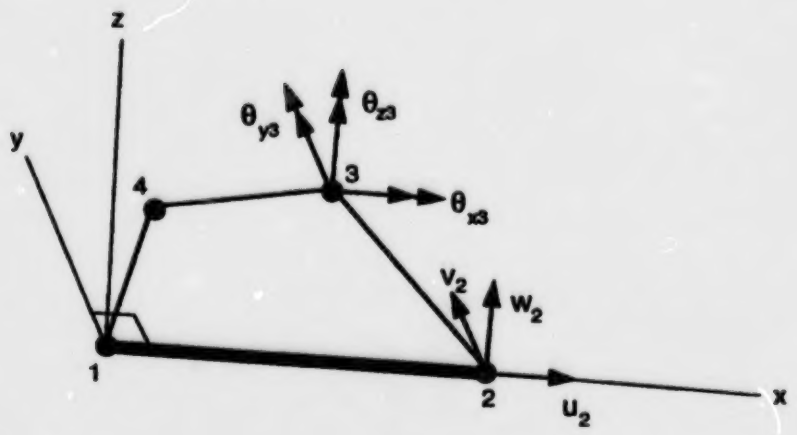

Figure 3: Geometric configuration and local frame of reference.

where x_i^e and y_i^e define the position of the ith element node, and where ψ_i are the bilinear shape functions given by

$$\begin{Bmatrix} \psi_1 \\ \psi_2 \\ \psi_3 \\ \psi_4 \end{Bmatrix} = \frac{1}{4} \begin{Bmatrix} (1-\xi)(1-\eta) \\ (1+\xi)(1-\eta) \\ (1+\xi)(1+\eta) \\ (1-\xi)(1+\eta) \end{Bmatrix}$$

or, in more compact form,

$$\psi_i = \frac{1}{4}(1+\xi_i\xi)(1+\eta_i\eta) \qquad \xi_i = \begin{matrix} -1, & i=1,4 \\ 1, & i=2,3 \end{matrix} \qquad \eta_i = \begin{matrix} -1, & i=1,2 \\ 1, & i=3,4 \end{matrix} \tag{22}$$

in which ξ and η are coordinates of the natural coordinate system depicted in Figure 4. The ith bilinear shape function has a unit value at the ith node and zero value at all other nodes, while varying linearly between the four nodes.

Three nodal displacement and three rotation variables are defined at each node and are referenced to the xyz system. In the isoparametric approach, the displacement functions u, v, w, θ_x and θ_y are interpolated using a linear combination of the same shape functions used to interpolate the position of interior points. The representation of the drilling freedom θ_z is special and is described separately in Section 4. As a general rule, the isoparametric approach leads to the numerically simplest of element formulations. The displacement fields are therefore written in the form

$$u \approx \sum_{i=1}^{4} \psi_i u_i^e \qquad v \approx \sum_{i=1}^{4} \psi_i v_i^e \qquad w \approx \sum_{i=1}^{4} \psi_i w_i^e \qquad \theta_x \approx \sum_{i=1}^{4} \psi_i \theta_{xi}^e \qquad \theta_y \approx \sum_{i=1}^{4} \psi_i \theta_{yi}^e \tag{23}$$

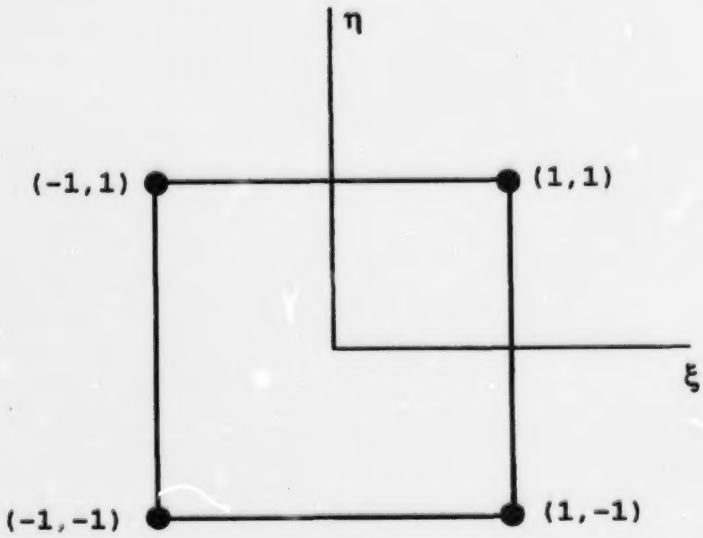

Figure 4: Natural coordinate system.

where u_i^e, v_i^e, w_i^e, θ_{xi}^e, θ_{yi}^e, are the displacements and rotations at the ith element node. In the isoparametric representation, displacement fields are compatible across element boundaries, regardless of their shape.

The displacement approximations (23) are now substituted into the membrane strain formula (9)

$$\epsilon^{(0)} = \sum_{i=1}^{4} \begin{bmatrix} \psi_{i,x} & 0 \\ 0 & \psi_{i,y} \\ \psi_{i,y} & \psi_{i,x} \end{bmatrix} \begin{Bmatrix} u_i^e \\ v_i^e \end{Bmatrix} = \sum_{i=1}^{4} \begin{bmatrix} S_u^{(i)} & S_v^{(i)} \end{bmatrix} \begin{Bmatrix} u_i^e \\ v_i^e \end{Bmatrix} = [S_m] \begin{Bmatrix} u^e \\ v^e \end{Bmatrix} \tag{24}$$

where

$$S_m = [S_u^{(1)}\ S_u^{(2)}\ S_u^{(3)}\ S_u^{(4)}\ S_v^{(1)}\ S_v^{(2)}\ S_v^{(3)}\ S_v^{(4)}] \qquad \{u^e\} = \{u_1^e\ \ldots u_4^e\}^T \qquad \{v^e\} = \{v_1^e\ \ldots v_4^e\}^T$$

On the other hand, substituting into the curvature formula gives

$$\epsilon^{(1)} = \sum_{i=1}^{4} \begin{bmatrix} \psi_{i,x} & 0 \\ 0 & -\psi_{i,y} \\ \psi_{i,y} & -\psi_{i,x} \end{bmatrix} \begin{Bmatrix} \theta_{xi}^e \\ \theta_{yi}^e \end{Bmatrix} = \sum_{i=1}^{4} \begin{bmatrix} S_u^{(i)} & -S_v^{(i)} \end{bmatrix} \begin{Bmatrix} \theta_{xi}^e \\ \theta_{yi}^e \end{Bmatrix} = \mathbf{S_b u_r} \tag{25}$$

where

$$\{\theta_x^e\} = \{\theta_{x1}^e\ \ldots \theta_{x4}^e\}^T \qquad \{\theta_y^e\} = \{\theta_{y1}^e\ \ldots \theta_{y4}^e\}^T$$

$$\mathbf{S_b} = [S_u^{(1)}\ S_u^{(2)}\ S_u^{(3)}\ S_u^{(4)}\ -S_v^{(1)}\ -S_v^{(2)}\ -S_v^{(3)}\ -S_v^{(4)}\ ] \qquad \mathbf{u_r} = \{\theta_x^e\ \theta_y^e\}^T \tag{26}$$

Similar substitutions could also be made to the transverse shear strain expressions (10). This leads to numerical difficulties, however, when the shell element becomes thin and the transverse shears must vanish. Because of the mixture of differentiated and non-differentiated terms, and because the same shape functions are used for each, it is not possible to satisfy the zero shear deformation condition everywhere in the element. In attempting to do this, the transverse deflection w is driven to zero, and the element "locks". The problem of shear locking in Mindlin shell elements has been commented on extensively. One popular way of avoiding it has been to use a reduced-order numerical integration for the shear strain energy terms [20]. Although this is effective at eliminating shear locking, it introduces zero-energy modes into the element which may have to be constrained to prevent spurious solutions. Another technique is to employ a different interpolation scheme for the shear strain energy, specially chosen so that the zero-strain condition can be correctly met for thin shells. The method used here is based on this concept and is described in detail in Section 6.

4 Drilling Degrees of Freedom

When using flat-facet plate/shell elements to represent three dimensional shell structures, the five DOF per node isoparametric framework outlined in the previous section is not adequate, as inconsistencies will arise when trying to assemble elements with different orientations in space. To correct for this an extra rotation coordinate, namely, the in-plane, or drilling coordinate, θ_z, must be supplied at each node. As the energy of in-plane rotations is not included in FSDT, it is usually seen to function simply as a place holder in the element assembly process. As such, drilling freedoms have generally been supplied with dummy stiffness values designed to prevent rigid body rotation in the sixth DOF [5].

An alternative approach is to provide the drilling freedoms with realistic shape functions and hence realistic stiffness values. The shape functions used for drilling freedoms in this study were developed by MacNeal and Harder [16] in a membrane element formulation, and were applied to flat-facet shell elements by Cook [15]. They are necessarily of higher-order than the bilinear shape functions, but still maintain inter-element compatibility. The technique is to replace the isoparametric expressions for u and v in (23) with the following two expressions:

$$\begin{aligned} u &= \sum_{i=1}^{4} \psi_i u_i^e + (y_{14}\psi_8 - y_{21}\psi_5)\theta_{z1} + (y_{21}\psi_5 - y_{32}\psi_6)\theta_{z2} \\ &\quad + (y_{32}\psi_6 - y_{43}\psi_7)\theta_{z3} + (y_{43}\psi_7 - y_{14}\psi_8)\theta_{z4} \end{aligned} \tag{27}$$

$$\begin{aligned} v &= \sum_{i=1}^{4} \psi_i v_i^e + (x_{41}\psi_8 - x_{12}\psi_5)\theta_{z1} + (x_{12}\psi_5 - x_{23}\psi_6)\theta_{z2} \\ &\quad + (x_{23}\psi_6 - x_{34}\psi_7)\theta_{z3} + (x_{34}\psi_7 - x_{41}\psi_8)\theta_{z4} \end{aligned} \tag{28}$$

where the first four ψ_i are the standard isoparametric bilinear shape functions, $x_{ij} = x_i - x_j$,

$y_{ij} = y_i - y_j$, and where

$$\psi_5 = \frac{1}{16}(1-\xi^2)(1-\eta) \qquad \psi_6 = \frac{1}{16}(1+\xi)(1-\eta^2)$$

$$\psi_7 = \frac{1}{16}(1-\xi^2)(1+\eta) \qquad \psi_8 = \frac{1}{16}(1-\xi)(1-\eta^2) \tag{29}$$

With these additional shape functions, the expression for membrane strain becomes

$$\epsilon^{(0)} = [S_m \; S_\theta] \left\{ \begin{array}{c} u^e \\ v^e \\ \theta_z^e \end{array} \right\} = \mathbf{S}_m \mathbf{u}_m \tag{30}$$

where S_θ is the matrix of strain coefficients associated with the drilling freedoms. Using (24) and generalising the above shape function expressions, this matrix can be written as

$$S_\theta = [S_{\theta 1} \; S_{\theta 2} \; S_{\theta 3} \; S_{\theta 4}] \tag{31}$$

where the submatrix for the ith node is

$$S_{\theta_i} = \left[\begin{array}{c} y_{ij}\psi_{j+4,x} - y_{ki}\psi_{i+4,x} \\ x_{ji}\psi_{j+4,y} - x_{ik}\psi_{i+4,y} \\ y_{ij}\psi_{j+4,y} - y_{ki}\psi_{i+4,y} + x_{ji}\psi_{j+4,x} - x_{ik}\psi_{i+4,x} \end{array} \right]$$

In this notation, $j = (i+2) \bmod 4 + 1$ and $k = i \bmod 4 + 1$.

5 Improving In-Plane Behaviour With Internal Shapes

A common problem with isoparametric shell elements is membrane shear locking. The four-node isoparametric membrane element, which uses the mid-plane strain in (24), is found to be too stiff in in-plane bending. A discussion by Cook et al. [6] on the subject shows that this is the result of a spurious in-plane shear strain that arises in pure bending. To some extent, this problem is lessened by associating meaningful shape functions to the drilling DOFs. It has been found, based on the recommendation in [15], that accuracy can be improved further by including quadratic shape functions associated with fictitious interior nodes, or "bubble" functions. The procedure is to supplement the u and v displacement functions as follows.

$$u = \text{Eq. (28)} + \phi_1(\xi)a \tag{32}$$

$$v = \text{Eq. (29)} + \phi_2(\eta)b \tag{33}$$

where $\phi_1(\xi) = (1-\xi^2)$, $\phi_2(\eta) = (1-\eta^2)$, and where a and b are internal degrees of freedom. Inclusion of these terms produces additional terms in the membrane strain expressions (30), becoming

$$\epsilon^{(0)} = \mathbf{S}_m \mathbf{u}_m + \mathbf{S}_d \mathbf{u}_d \tag{34}$$

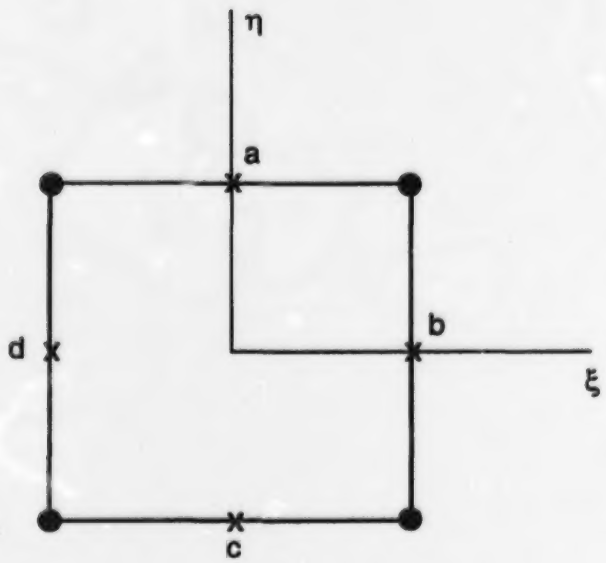

Figure 5: Mid-side points used to interpolate the transverse shear deformation.

where $\mathbf{u}_d = \{a\ b\}^T$, and

$$\mathbf{S}_d = \begin{bmatrix} \phi_{1,x} & 0 \\ 0 & \phi_{2,y} \\ \phi_{1,y} & \phi_{2,x} \end{bmatrix}$$

With non-rectangular elements, the quadratic shapes ϕ_1 and ϕ_2 are incompatible across element boundaries. This can cause patch test failures, among other problems, if appropriate precautions are not taken. Cook et al. [6] suggests a modified integration technique for terms dependent on the internal shape functions that enables the element to pass the patch tests. This is discussed further in Section 7.2.

6 Mixed Interpolation of Transverse Shear

As was noted in Section 3, transverse shear must be given a special treatment due to the problem of shear locking in thin shell elements. The approach used here first appears in the work of Hughes and Tezduyar [17] and was later generalized by Bathe and Dvorkin [14]. The general idea is illustrated in Figure 5. The transverse shear strains are first evaluated at the mid-side points a through d by interpolating the analytical expressions (10) with the standard bilinear shape functions. A second interpolation is then performed using the mid-side transverse shears and one-dimensional linear shape functions to give the shear strain at an arbitrary point within the element.

Mathematically, the procedure is carried out as follows. The mid-side shears are evaluated in the natural coordinate using the bilinear shape functions and the nodal displacements and rotations. This is written in matrix form as

$$\left\{ \begin{array}{c} \gamma^a_{\xi z} \\ \gamma^c_{\xi z} \\ \gamma^b_{\eta z} \\ \gamma^d_{\eta z} \end{array} \right\} = \sum_{i=1}^{4} \left[\begin{array}{ccc} \psi^a_{i,\xi} & 0 & \psi^a_i \\ \psi^c_{i,\xi} & 0 & \psi^c_i \\ \psi^b_{i,\eta} & -\psi^b_i & 0 \\ \psi^d_{i,\eta} & -\psi^d_i & 0 \end{array} \right] \left\{ \begin{array}{c} w^e_i \\ \theta^e_{xi} \\ \theta^e_{yi} \end{array} \right\} = [\mathbf{S}_w^{acbd} \; \mathbf{S}_r^{acbd}] \left\{ \begin{array}{c} \mathbf{u}_w \\ \mathbf{u}_r \end{array} \right\} \tag{35}$$

where $\mathbf{u}_w \equiv w^e$ and $\mathbf{u}_r$ is given in (26). $\mathbf{S}_w^{acbd}$ and $\mathbf{S}_r^{acbd}$ are partitions of the coefficient matrix associated with the transverse deflection and rotations, respectively. The shear strains at an arbitrary interior point are then obtained, also in natural coordinates, as

$$\gamma_{\xi z} = \frac{1}{2}(1+\eta)\gamma^a_{\xi z} + \frac{1}{2}(1-\eta)\gamma^c_{\xi z} \tag{36}$$

$$\gamma_{\eta z} = \frac{1}{2}(1+\xi)\gamma^d_{\eta z} + \frac{1}{2}(1-\xi)\gamma^b_{\eta z} \tag{37}$$

The shear strains are now transformed to the local xy coordinate system. Applying the general metric tensor transformation [29] gives the transverse shear in natural coordinates as

$$\left\{ \begin{array}{c} \gamma_{\xi z} \\ \gamma_{\eta z} \end{array} \right\} = \left[\begin{array}{cc} x_{,\xi} & y_{,\xi} \\ x_{,\eta} & y_{,\eta} \end{array} \right] \left\{ \begin{array}{c} \gamma_{xz} \\ \gamma_{yz} \end{array} \right\} = J \left\{ \begin{array}{c} \gamma_{xz} \\ \gamma_{yz} \end{array} \right\} \tag{38}$$

where J denotes the Jacobian matrix. Inverting this transformation, and combining it with (35) and (36) gives the final expression for the shear strain as,

$$\left\{ \begin{array}{c} \gamma_{xz} \\ \gamma_{yz} \end{array} \right\} = J^{-1}\Gamma(\xi,\eta)[\mathbf{S}_w^{acbd} \; \mathbf{S}_r^{acbd}] \left\{ \begin{array}{c} \mathbf{u}_w \\ \mathbf{u}_r \end{array} \right\} \tag{39}$$

where

$$\Gamma(\xi,\eta) = \left[\begin{array}{cccc} \frac{1}{2}(1+\eta) & \frac{1}{2}(1-\eta) & 0 & 0 \\ 0 & 0 & \frac{1}{2}(1+\xi) & \frac{1}{2}(1-\xi) \end{array} \right]$$

In gathering together all the terms it is convenient to partition them so as to separate terms related to $\mathbf{u}_w$ from those related to the rotation coordinates $\mathbf{u}_r$. Hence the final expression for shear strain is

$$\gamma = [\mathbf{S}_w \; \mathbf{S}_r] \left\{ \begin{array}{c} \mathbf{u}_w \\ \mathbf{u}_r \end{array} \right\} \tag{40}$$

where $\mathbf{S}_w = J^{-1}\Gamma(\xi,\eta)\mathbf{S}_w^{acbd}$ and $\mathbf{S}_r = J^{-1}\Gamma(\xi,\eta)\mathbf{S}_r^{acbd}$.

7 Element Stiffness Formulation

7.1 Flat Element Stiffness Matrix

The element stiffness is obtained from the variational form (13) and from the previously given expressions for strains and the stress resultants. By applying the FSDT constitutive

equations (14,15) to (13) the variational form becomes

$$0 = \int_{\Omega^e} \left[\{\delta\epsilon^{(0)}\}^T \{A\epsilon^{(0)} + B\epsilon^{(1)}\} + \{\delta\epsilon^{(1)}\}^T \{B\epsilon^{(0)} + D\epsilon^{(1)}\} + \{\delta\gamma\}^T E\{\gamma\} - q\delta w \right] \mathrm{d}x\,\mathrm{d}y \tag{41}$$

The strain vectors $\epsilon^{(0)}$, $\epsilon^{(1)}$, γ and their virtual counterparts are now replaced with their interpolated forms (34), (25) and (40). The virtual displacement δw is expanded using the bilinear shape functions, becoming $\{\delta \mathbf{u}_w\}^T\{\psi\}$. The resulting equation is

$$\begin{aligned}
0 &= \int_{\Omega^e} \{\delta \mathbf{u}_m\}^T \left(\mathbf{S}_m^T[A](\mathbf{S}_m \mathbf{u}_m + \mathbf{S}_d \mathbf{u}_d) + \mathbf{S}_m^T[B]\mathbf{S}_b \mathbf{u}_r \right) \mathrm{d}x\,\mathrm{d}y \\
&+ \int_{\Omega^e} \{\delta \mathbf{u}_d\}^T \left(\mathbf{S}_d^T[A](\mathbf{S}_m \mathbf{u}_m + \mathbf{S}_d \mathbf{u}_d) + \mathbf{S}_d^T[B]\mathbf{S}_b \mathbf{u}_r \right) \mathrm{d}x\,\mathrm{d}y \\
&+ \int_{\Omega^e} \{\delta \mathbf{u}_r\}^T \left(\mathbf{S}_b^T[B](\mathbf{S}_m \mathbf{u}_m + \mathbf{S}_d \mathbf{u}_d) + \mathbf{S}_b^T[D]\mathbf{S}_b \mathbf{u}_r \right) \mathrm{d}x\,\mathrm{d}y \\
&+ \int_{\Omega^e} \left[\left\{ \begin{array}{c} \delta \mathbf{u}_w \\ \delta \mathbf{u}_r \end{array} \right\}^T [\mathbf{S}_w\ \mathbf{S}_r]^T [E] [\mathbf{S}_w\ \mathbf{S}_r] \left\{ \begin{array}{c} \mathbf{u}_w \\ \mathbf{u}_r \end{array} \right\} - q\{\delta \mathbf{u}_w\}^T\{\psi\} \right] \mathrm{d}x\,\mathrm{d}y
\end{aligned}$$

By allowing each of the virtual displacements in $\delta \mathbf{u}_m$, $\delta \mathbf{u}_d$, $\delta \mathbf{u}_w$, and $\delta \mathbf{u}_r$ to vary independently, six equations are generated from the single variational equation. These separate out as follows

$$\begin{aligned}
\mathbf{K}_{mm}\mathbf{u}_m + \mathbf{K}_{md}\mathbf{u}_d + \mathbf{K}_{mr}\mathbf{u}_r &= 0 \\
\mathbf{K}_{md}^T\mathbf{u}_m + \mathbf{K}_{dd}\mathbf{u}_d + \mathbf{K}_{dr}\mathbf{u}_r &= 0 \\
\mathbf{K}_{ww}\mathbf{u}_w + \mathbf{K}_{wr}\mathbf{u}_r &= F_w \\
\mathbf{K}_{mr}^T\mathbf{u}_m + \mathbf{K}_{dr}^T\mathbf{u}_d + \mathbf{K}_{rw}^T\mathbf{u}_w + \mathbf{K}_{rr}\mathbf{u}_r &= 0
\end{aligned} \tag{42}$$

where

$$\mathbf{K}_{mm} = \int_{\Omega^e} \mathbf{S}_m^T[A]\mathbf{S}_m \,\mathrm{d}x\,\mathrm{d}y \qquad \mathbf{K}_{md} = \int_{\Omega^e} \mathbf{S}_m^T[A]\mathbf{S}_d \,\mathrm{d}x\,\mathrm{d}y \tag{43}$$

$$\mathbf{K}_{dd} = \int_{\Omega^e} \mathbf{S}_d^T[A]\mathbf{S}_d \,\mathrm{d}x\,\mathrm{d}y \qquad \mathbf{K}_{dr} = \int_{\Omega^e} \mathbf{S}_d^T[B]\mathbf{S}_b \,\mathrm{d}x\,\mathrm{d}y \tag{44}$$

$$\mathbf{K}_{mr} = \int_{\Omega^e} \mathbf{S}_m^T[B]\mathbf{S}_b \,\mathrm{d}x\,\mathrm{d}y \qquad \mathbf{K}_{rr} = \int_{\Omega^e} [\mathbf{S}_b^T[D]\mathbf{S}_b + \mathbf{S}_r^T[E]\mathbf{S}_r] \,\mathrm{d}x\,\mathrm{d}y \tag{45}$$

$$\mathbf{K}_{ww} = \int_{\Omega^e} \mathbf{S}_w^T[E]\mathbf{S}_w \,\mathrm{d}x\,\mathrm{d}y \qquad \mathbf{K}_{wr} = \int_{\Omega^e} \mathbf{S}_w^T[E]\mathbf{S}_r \,\mathrm{d}x\,\mathrm{d}y \tag{46}$$

$$F_w = \int_{\Omega^e} q\{\phi\} \,\mathrm{d}x\,\mathrm{d}y \tag{47}$$

The terms $\mathbf{K}_{mm}$, $\mathbf{K}_{dd}$, and $\mathbf{K}_{md}$ are component matrices of the element stiffness that relate to in-plane deformation only. They are of size 12×12, 2×2, and 12×2, respectively. $\mathbf{K}_{rr}$, $\mathbf{K}_{ww}$, and $\mathbf{K}_{wr}$ are the component matrices governing out-of-plane deformation (i.e., bending and transverse shear). These matrices are of size 8×8, 12×12, and 12×8, respectively. Coupling between the in-plane and out-of-plane deformation is controlled by

the two matrices $\mathbf{K}_{mr}$ and $\mathbf{K}_{dr}$, which are of size 12×8, 2×8, respectively. Both of these are zero when the laminate coupling matrix $[B]$ is equal to zero.

The term F_w is the 4×1 load vector that occurs as a result of a surface pressure on the face of the element. Additional force terms could also be derived by considering body loads and other surface and edge tractions. Also omitted are the edge forces and moments imposed by adjacent elements. These terms need not be considered explicitly as they invariably cancel out with one another when inter-element equilibrium is satisfied during element assembly.

Internal degrees $\mathbf{u}_d$ are not affected by external loading or by inter-element compatibility and equilibrium requirements. Thus, the right-hand side of the second equation in (42) will always be zero. Assuming $\mathbf{K}_{dd}$ to be nonsingular, $\mathbf{u}_d$ can then be written as

$$\mathbf{u}_d = -\mathbf{K}_{dd}^{-1}\left(\mathbf{K}_{md}^T\mathbf{u}_m + \mathbf{K}_{dr}\mathbf{u}_r\right) \tag{48}$$

With this equation, all terms related to $\mathbf{u}_d$ can be eliminated from the (42) by the usual static condensation procedure. Once this is done, the entire element stiffness matrix can be written as

$$\mathbf{K} = \begin{bmatrix} \mathbf{K}_{mm} - \mathbf{K}_{md}\mathbf{K}_{dd}^{-1}\mathbf{K}_{md}^T & 0 & \mathbf{K}_{mr} - \mathbf{K}_{md}\mathbf{K}_{dd}^{-1}\mathbf{K}_{dr} \\ 0 & \mathbf{K}_{ww} & \mathbf{K}_{wr} \\ \mathbf{K}_{mr}^T - \mathbf{K}_{dr}^T\mathbf{K}_{dd}^{-1}\mathbf{K}_{md}^T & \mathbf{K}_{wr}^T & \mathbf{K}_{rr} - \mathbf{K}_{dr}^T\mathbf{K}_{dd}^{-1}\mathbf{K}_{dr} \end{bmatrix} \tag{49}$$

The above formulation renders a stiffness matrix in the local coordinate system of the element. Before the elements can be assembled into the global equations of the structural system, the element matrices and load vectors must first be transformed to the global coordinate system. This is a simple matter of applying the standard force and displacement transformation procedures.

7.2 Numerical Integration

The integrals in (43–47) are calculated by Gaussian quadrature in the natural coordinate system. The first step is to make the substitution $\mathrm{d}x\,\mathrm{d}y = \det J\,\mathrm{d}\xi\,\mathrm{d}\eta$, where $\det J$ is the determinant of the Jacobian matrix defined in (38). Since derivatives of quantities with respect to x and y are calculated in terms of derivatives in terms of ξ and η, all the terms in the above integrands are in the following general form:

$$I = \int_{\Omega^e} F(\xi,\eta)\,\mathrm{d}x\,\mathrm{d}y = \int_{\Omega^e} F(\xi,\eta)\det J\,\mathrm{d}\xi\,\mathrm{d}\eta$$

In Gaussian quadrature, this integral is replaced by the following double summation:

$$I = \sum_{j=1}^{M}\sum_{k=1}^{N} F(\xi_j,\eta_k)\,W_j W_k \det J(\xi_j,\eta_k)$$

where ξ_j, η_k are discrete points where the integrands are evaluated, and W_j, W_k are weights associated with particular integration points. In this study, $M = N = 2$ is used for nearly all the integrals, in which the positions of the four integration points are $\xi, \eta = \pm 0.5773502692$,

and $W = 1.0$ at all points. The exceptions are the matrices relating to the internal shape functions: $\mathbf{K}_{dd}$, $\mathbf{K}_{md}$ and $\mathbf{K}_{rd}$. For these the modified integration scheme suggested by Cook et al. [6] is used. In this approach, the Jacobian used in both $\mathbf{S}_d$ and $\det J$ is evaluated at $\xi, \eta = 0$. All the other terms in these integrals are evaluated at the 2×2 integration points.

7.3 Removal of Rigid Body Mechanism in Drilling DOF [15]

The formulation of the membrane strain drilling freedoms presented in Section 4 has a zero-energy mode in which all four drilling freedoms take identical values. To control this "rigid body" mode, the $\mathbf{K}_{mm}$ portion of the stiffness matrix is supplemented by a small additional matrix in which this mode is suppressed. The supplementary matrix is obtained by considering in turn the four overlapping subtriangles defined by the element node combinations 123, 234, 341, 412. In the first case, a stiffness submatrix is defined by

$$\mathbf{k}_s = 10^{-6} S \sqrt{A_{11} A_{22}}\, \mathbf{R}^T \mathbf{R}$$

where S is the are of the element mid-plane, A_{11} and A_{22} are the (1,1) and (2,2) components of the laminate $[A]$ matrix, and

$$\mathbf{R} = \begin{bmatrix} \frac{x_{23}}{4S} & \frac{y_{23}}{4S} & -\frac{1}{3} & \frac{x_{31}}{4S} & \frac{y_{31}}{4S} & -\frac{1}{3} & \frac{x_{12}}{4S} & \frac{y_{12}}{4S} & -\frac{1}{3} \end{bmatrix}$$

The elements of $\mathbf{R}$ operate on DOF $\{u_1\ v_1\ \theta_{z1}\ u_2\ v_2\ \theta_{z2}\ u_3\ v_3\ \theta_{z3}\ \}$. Similarly, $\mathbf{k}_s$ matrices can be generated for the other three subtriangles. All four are assembled in a 12×12 matrix and are added to $\mathbf{K}_{mm}$. The factor of 10^{-6} is chosen arbitrarily; any number producing relatively small stiffness values would work as well.

7.4 Correction for Warping

The flat-facet quadrilateral element can be highly inaccurate when the element is warped, i.e., when its four corner nodes do not all lie in the same plane. Consequently, a modification to the element is required for it to behave correctly in this situation.

The warping correction method developed by Naganarayana and Prathap [30] is used in the present work. It is based on the observation that the usual nodal membrane forces that occur in the flat element will produce an unequilibrated moment in the warped configuration. The general idea is to put the element back into equilibrium by introducing forces in the local z direction that counter-balance the moment due to the membrane forces. As shown in Figure 6, the warping can be quantified as a distance H between the nodes and a corner of the unwarped mid-plane. The sign of H alternates from node to node, but the magnitude is the same. Establishing the local coordinate system of the element with reference to the middle plane, a transformation is then developed between the nodal forces of the unwarped element and those of warped element. In this it is assumed that only forces in the z-direction are affected by the warping.

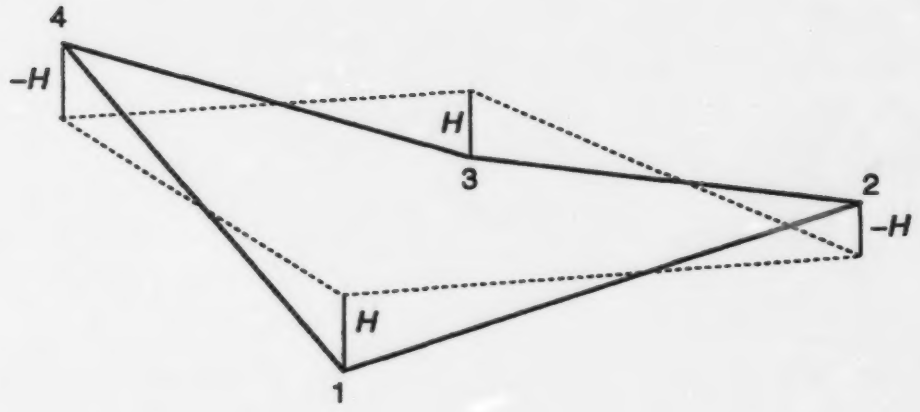

Figure 6: Characterization of warping as a distance H from an unwarped middle plane.

Considering only nodal forces acting on the element, the equations of force and moment equilibrium are obtained as

$$\sum_{i=1}^{4} f_{xi} = 0 \qquad \sum_{i=1}^{4} f_{yi} = 0 \qquad \sum_{i=1}^{4} f_{zi} = 0 \tag{50}$$

$$\sum_{i=1}^{4} f_{yi} x_i = \sum_{i=1}^{4} f_{xi} y_i \qquad \sum_{i=1}^{4} f_{zi} x_i = \sum_{i=1}^{4} f_{xi} z_i \qquad \sum_{i=1}^{4} f_{zi} y_i = \sum_{i=1}^{4} f_{yi} z_i \tag{51}$$

Using the last equation of (50) and the second and third of (51), three equations are obtained in the four unknowns to be determined (f_{zi}). The fourth equation is obtained from virtual work considerations and is given as [30]

$$\sum_{i=1}^{4} f_{zi} z_i = 0 \tag{52}$$

Solving these for f_{zi} gives

$$f_z = T_z^{-1} T_x f_x + T_z^{-1} T_y f_y \tag{53}$$

where

$$T_x = \begin{bmatrix} 0 & 0 & 0 & 0 \\ z_1 & z_2 & z_3 & z_4 \\ 0 & 0 & 0 & 0 \\ 0 & 0 & 0 & 0 \end{bmatrix} \qquad T_y = \begin{bmatrix} 0 & 0 & 0 & 0 \\ 0 & 0 & 0 & 0 \\ z_1 & z_2 & z_3 & z_4 \\ 0 & 0 & 0 & 0 \end{bmatrix} \qquad T_z = \begin{bmatrix} 1 & 1 & 1 & 1 \\ x_1 & x_2 & x_3 & x_4 \\ y_1 & y_2 & y_3 & y_4 \\ z_1 & z_2 & z_3 & z_4 \end{bmatrix}$$

This gives the following transformation between the forces on unwarped element (f_{xp}, f_{yp}, f_{zp}) and those of the real element:

$$\begin{Bmatrix} f_x \\ f_y \\ f_z \end{Bmatrix} = \begin{bmatrix} I & 0 & 0 \\ 0 & I & 0 \\ T_x^{-1}T_z & T_x^{-1}T_y & I \end{bmatrix} \begin{Bmatrix} f_{xp} \\ f_{yp} \\ f_{zp} \end{Bmatrix} = T_f f_p \tag{54}$$

in which T_f is a 12×12 matrix.

A complete transformation for all 24 DOF is obtained by inserting the identity matrix for the moment terms. Denoting $\mathbf{f}$ and $\mathbf{f}_p$ as the 24×1 nodal force and moment vectors for the warped and unwarped elements, respectively, the total transformation is

$$\mathbf{f} = \begin{bmatrix} T_f & 0 \\ 0 & I \end{bmatrix} \mathbf{f}_p = \mathbf{T}_e^T \mathbf{f}_p \tag{55}$$

Once the element stiffness is computed for the unwarped configuration, according to the procedures described in the previous sections, the warped element stiffness is then obtained as

$$\mathbf{K}' = \mathbf{T}_e^T \mathbf{K} \mathbf{T}_e \tag{56}$$

where the prime denotes the warping compensated stiffness. The transformation for warping correction must be carried out before the transformation of the element matrix to global coordinates.

8 Implementation and Solution

The element formulation described in the previous sections has been implemented in a programme, FELAM, which was recently developed at DREA for finite element analysis of laminated plate and shell structures. The programme has been coded in C++ using the object-oriented methodology, and incorporates many attractive features such as polymorphism, data encapsulation, dynamic memory allocation, and operator overloading. The program has been developed both as a means of acquiring an in-house composite analysis capability, and also as a research platform for composite and finite-element related numerical methods. At present, the program is still in a preliminary stage of development, and is only capable of linear static and first-ply failure analysis. Solution of the global equations of the structual system is performed using the direct LU-decomposition method. As the solver does not take account either of the symmetry or the sparseness of the system equations, it is limited to structural models of relatively small size. The largest problem size that has been successfully solved to date is 256 nodes. Given a physical memory of 96 Megabytes, which is typical for current PC technology, the practical limit in double precision arithmetic would be about 500 nodes.

Implementing the present element formulation in the VAST programme would require significant improvements in the material modelling capabilities of the latter. Originally, the

VAST programme was not designed with composite structures in mind, and its composite material capabilities were only added later after the programme's structure had become fixed. As a result, there exist a number of inconsistencies in VAST's specification of material properties that can make the programme awkward to use. In particular, composite elements in VAST require the lay up sequence and layer orientations to be defined for each element individually. This is a wasteful practice, since a large number of elements will typically share the same layup sequence. In the FELAM programme, layer properties and laminates are defined in a materials input file and are each identified by a unique character string. An individual element can then be associated with a laminate by using just the string identifier and a single orientation angle that aligns the element with the laminate reference frame.

9 Post-Computation of Stresses

Once nodal displacements and rotations have been solved, stress computation can proceed on a layer-by-layer, element-by-element basis. The first step is to compute strains for each layer in an element using Equations (8), (24), (25), and (40). Since the strains are continuous functions of the spatial variables within a layer of an element, it is only practical to calculate strain and hence, stress, at selected points in the element. The locations for the most accurate stress computations are known to be the Gauss integration points one order lower than those used to compute the element stiffness. So, for example, if the stiffness terms are evaluated with 2×2 Gauss quadrature, then stresses should be computed at the 1×1 Gauss point. Thus, for the composite shell element considered here, all strains and stress are evaluated at $\xi = 0, \eta = 0$.

Typically, a single point on the top and bottom of each layer is sufficient for the in-plane strain components. For example, the strains at the bottom and top of the kth layer are given by

$$\epsilon^{(k)}_{bottom} = \epsilon^{(0)}(0,0) + z_k \epsilon^{(1)}(0,0) \qquad \epsilon^{(k)}_{top} = \epsilon^{(0)}(0,0) + z_{k+1} \epsilon^{(1)}(0,0)$$

where (0,0) indicates the position in natural coordinates where the shape function derivatives are evaluated. The transverse strain components are obtained directly from Equation (40) with $\xi = 0, \eta = 0$, and are assumed constant through the thickness of the laminate.

For a layer of given orientation θ with respect to the element coordinate system, the strain is obtained in fibre-matrix coordinates as

$$\overline{\epsilon} = \mathbf{T}\epsilon \tag{57}$$

where $\mathbf{T}$ is given in (6). Stresses can now be calculated at the same locations where strains are computed. In the fibre-matrix coordinate system these are obtained by

$$\overline{\sigma} = \mathbf{C}\overline{\epsilon} \tag{58}$$

Stresses can be obtained in the element coordinate system either directly from (4) or simply by multiplying $\overline{\sigma}$ by the transpose of $\mathbf{T}$.

Test	Thickness	Quantity	% Error
In-plane Stretching	1.0	u_{max}	3×10^{-10}
In-plane Shear	1.0	v_{max}	-1×10^{-4}
Bending	0.001	w_{max}	-1×10^{-5}
Bending	1.0	w_{max}	2×10^{-8}
Out-of-plane Shear	0.001	w_{max}	2×10^{-10}
Out-of-plane Shear	1.0	w_{max}	2×10^{-7}
Twisting	0.001	w_{max}	-1×10^{-5}
Twisting	1.0	w_{max}	1×10^{-9}

Table 1: Patch test results.

10 Numerical Validation

10.1 Patch Tests

An important test for any new element is whether it can predict constant strain states. The ability to do so guarantees that the element will converge to the exact answer in any arbitrary stress state as the mesh is refined. Tests for constant strain state are known as patch tests [5]. Five different patch tests are needed to test the quadrilateral shell element: (1) in-plane stretching, (2) in-plane shear, (3) bending, (4) out-of-plane shear, and (5) twisting. The required loading conditions to produce each of these on a square patch are illustrated in Figure 7. Analytical solutions are available in all five cases, making it easy to verify if the correct constant strain state is predicted. If it is able to predict the analytical solution "exactly", i.e. within the limit imposed by numerical noise, the element is said to pass the patch test. Irons and Ahmad [31] suggest that six decimals of accuracy is sufficient for a passing grade.

The meshed patch consists of five non-rectangular elements as shown in Figure 8. A laminate comprised of a single layer of isotropic material is used, in which the material properties are $E = 2.1 \times 10^6$ and $\nu = 0.3$. For the last three patch tests, two different thickness values are used (1.0 and 0.001) to test for the occurence of shear locking. In addition to the constraints indicated in Figure 7, the in-plane rotations at the four corners are also constrained to prevent unintended deformations from occurring due to the concentrated loads. Results for all cases are given in Table 1 as a precentage error of the analytical results for the selected quantities indicated in the table. The shell element passes all of the patch tests, although the in-plane shear case is of borderline accuracy. Degradation of the results at the smaller thickness due to shear locking is negligible.

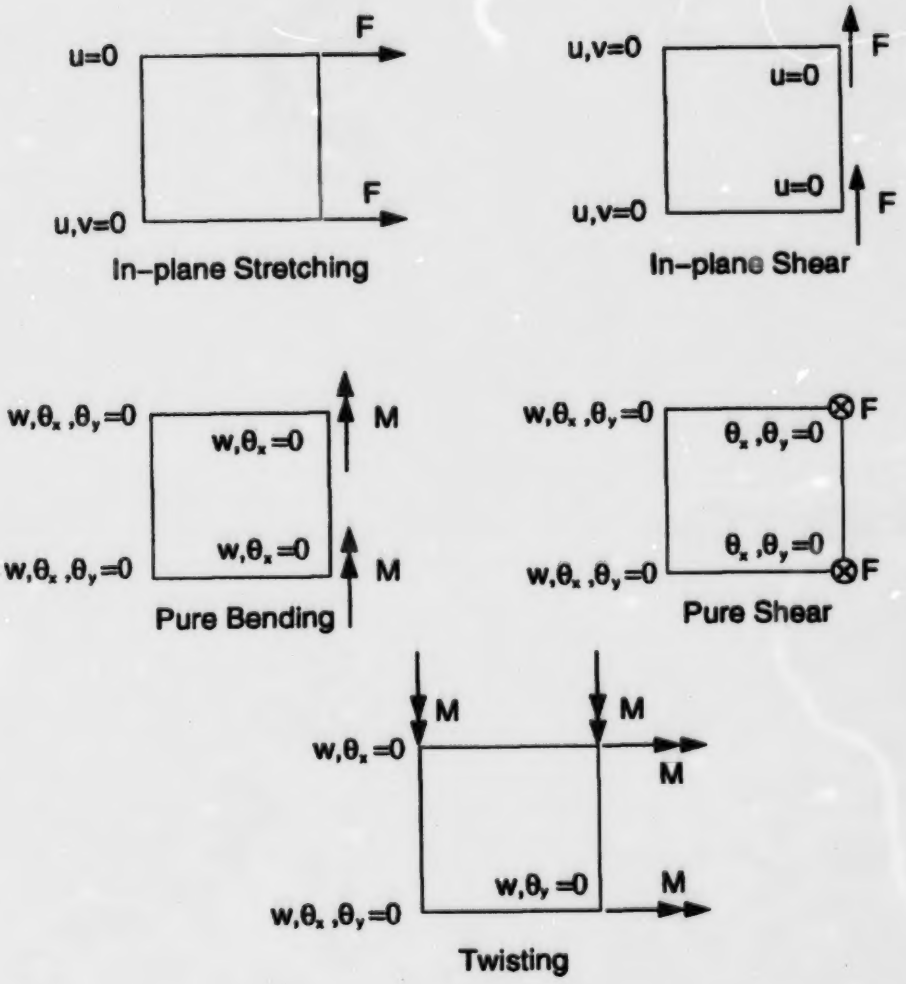

Figure 7: Five patch tests used to verify convergence of a four-node shell element [29].

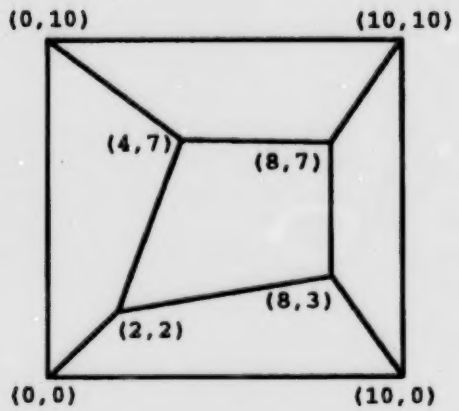

Figure 8: Five element mesh used for all patch tests.

10.2 Obstacle Course Example Problems

The four standard 'obstacle course' test problems proposed by Belytschko and Wong [12] plus an additional cantilevered beam problem proposed by Cook [15] are used here to evaluate the performance of the Shell4 element in structures with isotropic material properties. In these examples, element material properties are defined as a laminate comprised of a single, isotropic layer. For comparison purposes, VAST and ANSYS results are also obtained using quadrilateral shell elements. The VAST shell element (IEC = 5) is based on the degenerate solid formulation of Bathe and Dvorkin [14]; the ANSYS shell element (SHELL43) is based on a similar degenerate solid formulation.

10.2.1 Cantilevered Beam

The cantilevered beam in Figure 9 is put into bending by oppositely directed point loads applied at its end. The effect of mesh distortion on the results is investigated with the second of the two meshes depicted in the figure. Results for the two cases are given in Table 2, where the vertical tip deflection is given as a ratio of the theoretical value of 0.018. Although the accuracy of all three elements suffers through distortion of the mesh, the Shell4 element is much less sensitive in this regard than either the VAST or ANSYS elements. This can be attributed to the use in Shell4 of drilling freedoms with realistic shape functions and stiffness coefficients. The other two elements use placeholder-type drilling freedoms with artificial stiffness.

Example	Mesh	Shell4	VAST	ANSYS
Cantilevered Beam	regular	0.9999	1.0000	0.9999
	distorted	0.8745	0.1017	0.0472
Twisted Beam	4 × 2	0.7932	0.9886	0.9870
(In-plane Shear)	8 × 2	0.8814	1.006	0.9923
	12 × 2	0.9593	0.9971	0.9948
TwistedBeam	4 × 2	0.8038	0.9031	0.9259
(Out-of-plane Shear)	8 × 2	0.9065	0.9555	1.0063
	12 × 2	1.0196	0.9875	1.0218
Scordelis-Lo Roof	2 × 2	1.376	1.377	1.380
	4 × 4	1.048	1.109	1.047
	8 × 8	1.006	1.065	1.006
Pinched Cylinder	2 × 2	0.0351	0.0416	0.0621
	4 × 4	0.3764	0.3878	0.3976
	8 × 8	0.7451	0.7541	0.7594
	16 × 16	0.9283	0.9311	0.9336
Hemispherical Shell	2 × 2	0.0378	0.8591	0.8621
	4 × 4	0.3413	0.9979	0.9550
	8 × 8	0.9380	0.9934	0.9910
	16 × 16	0.9668	0.9947	0.9940

Table 2: Finite element results for the obstacle course example problems (displacements expressed as a ratio of the theoretical values).

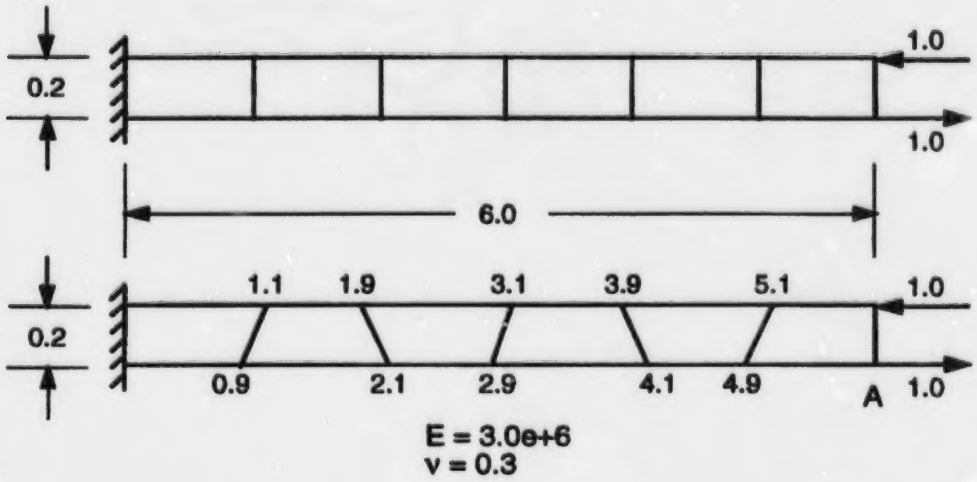

Figure 9: Regular and distorted meshes for a cantilevered beam (not to scale).

10.2.2 Twisted Beam

This problem serves to test the element in a warped configuration. The cantilevered beam in Figure 10 undergoes 90 degrees of twist over its length. A unit load is applied in each of the transverse directions. The theoretical solutions for the deflections at A are 0.005424 (in-plane shear) and 0.001754 (out-of-plane shear), where the deflection is in both cases measured in the direction of the loading. Finite element results are given in Table 2 for three different meshes. Shell4 converges more slowly than either the VAST or the ANSYS elements. Without the warping correction, the displacements are about one-quarter to one-half the size. Shell4 does not appear to work as well as the other two elements in a warped configuration.

10.2.3 Scordelis-Lo Roof

In this problem, illustrated in Figure 11, a cylindrical roof is simply supported at its curved ends and is loaded by its own weight. Using symmetry conditions at the edges, only one-quarter of the model is meshed with $N \times N$ elements. The theoretical midside vertical displacement (point A) quoted by MacNeal and Harder [32] is 0.3086. They also state that most finite elements converge to a slightly lower value of 0.3024, and use this as their normalization constant. This convention will also be adopted in the present study. Results for three levels of mesh refinement are given in Table 2. There are no significant differences among the three elements.

Figure 10: Twisted cantilever beam with a 4×2 mesh.

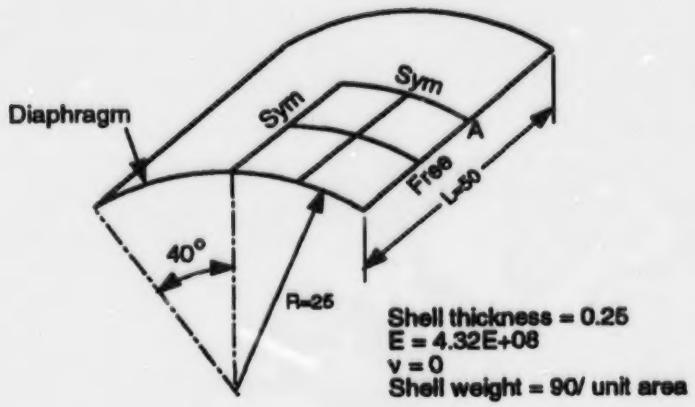

Figure 11: Scordelis-Lo roof problem showing a 2×2 meshed region.

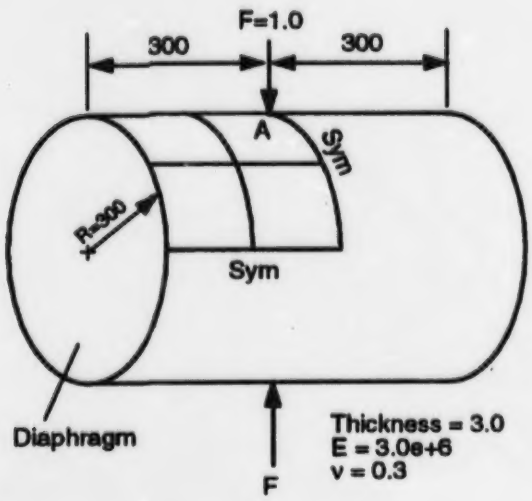

Figure 12: One-eighth model of a cylindrical shell with a 2×2 mesh.

10.2.4 Pinched Cylinder

The cylindrical shell in Figure 12 is supported at each end by rigid diaphragms which only allow displacement in the axial direction. Point loads are applied normal to the surface of the cylinder at two points on a line passing through the centre, so that the cylinder is 'pinched'. One-eighth of the shell surface is meshed as shown in the figure, with appropriate symmetry conditions applied to the edges. The theoretical displacement at the point of loading (A) is 0.18248×10^{-4} [14]. Finite element results for the loading point deflections are given in Table 2 for three different meshes. The results are very similar for all three element types.

10.2.5 Hemispherical Shell

The hemispherical shell in Figure 13 is pinched in the y direction and pulled in the x direction by forces of unit magnitude. One quarter of the shell is meshed with appropriate symmetry conditions applied at the edges. The hole of radius 0.175 is introduced in the crown of the hemisphere to avoid degeneracy of the elements. The theoretical displacement at point A is quoted in [32] as 0.0924. Results for three levels of mesh refinement are given in Table 2. The Shell4 element appears to be exceptionally stiff with the coarser meshes.

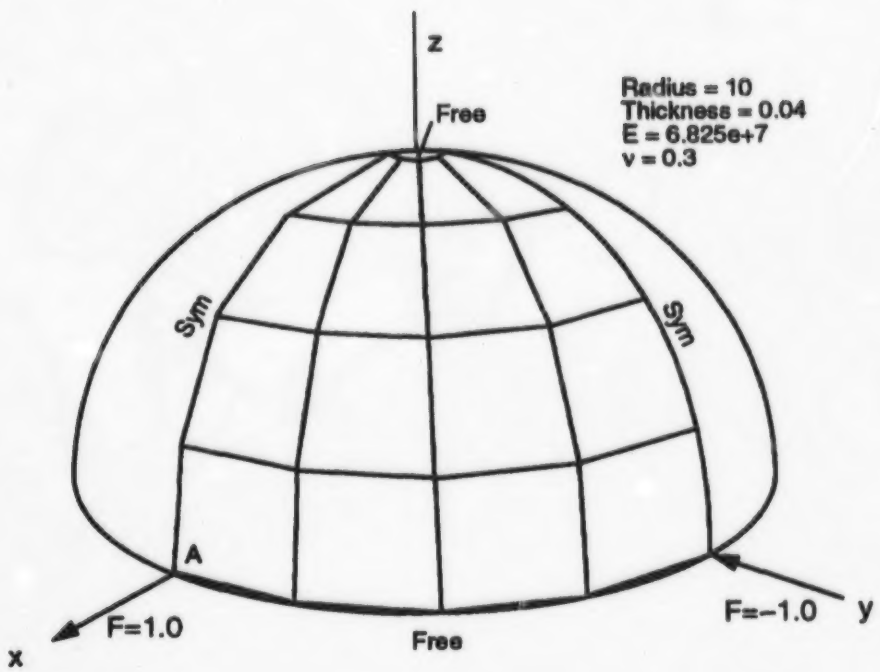

Figure 13: One-quarter model of a hemispherical shell with a 4 × 4 mesh.

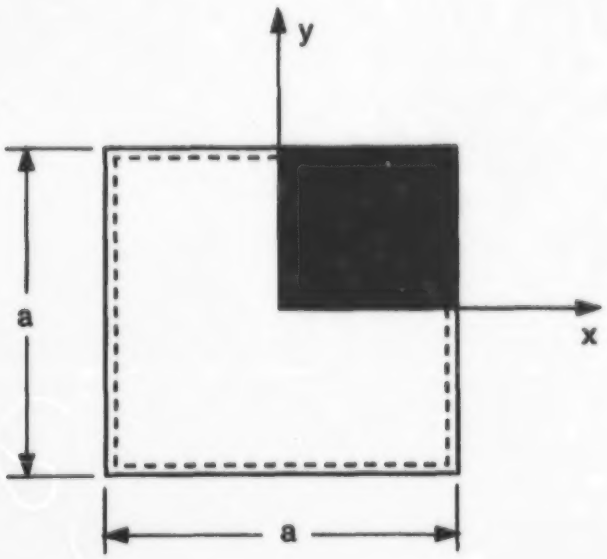

Figure 14: Modelled region for simply supported plates.

10.3 Composite Plate Examples

10.3.1 Thin Plate Under Uniform Loading

Reddy [26] previously used four examples of square laminated plates with uniform loading and simply supported boundary conditions to compare analytical and finite element results. The same examples are used here to validate the composite material capabilities of the Shell4 element. Also included are results obtained with the ANSYS eight-node composite element SHELL99. No comparable element currently exists in the VAST programme. Reddy's analytical results repeated here are obtained from classical laminate theory, and therefore only apply for thin laminates.

The basic simply supported arrangement for all plates is shown in Figure 14. The symmetry of the problems is exploited by analysing only one-quarter of the plate, with appropriate boundary conditions applied to the $x = 0$ and $y = 0$ edges. Table 3 lists two different boundary conditions investigated here for enforcing symmetry. Transverse displacement and normal rotations are suppressed at the simply supported edges.

Results for four different laminates using the laminar properties $E_1/E_2 = 25$, $G_{12} = 0.5E_2$, and $\nu_{12} = 0.25$ are given in Table 4. The layer thicknesses are given by $h_n = h/n$, where n is the total number of layers, and h is the overall thickness. Table 5 gives the normalised quantities and locations where the deflections and stresses were evaluated in both the Shell4 and Reddy's analytical results. In ANSYS, stresses are reported at nodes rather than Gauss points. Therefore in the ANSYS results, σ_{xx} and σ_{yy} are nodal values

B.C.	$x = 0$		$y = 0$	
SS-1	$u = 0$	$\theta_y = 0$	$v = 0$	$\theta_x = 0$
SS-2	$v = 0$	$\theta_y = 0$	$u = 0$	$\theta_x = 0$

Table 3: Boundary conditions for enforcing symmetry.

calculated on the top surface at the centre of the plate, while τ_{xy} was calculated on the bottom surface at the upper right corner node.

Good comparisons with the analytical results were obtained by using very thin laminates in the FE models (the total thickness was $a/4000$ in all cases). This effectively eliminated transverse shear from the analysis, and yet no evidence of locking was observed in the Shell4 element. The Shell4 results compare extremely well with the ANSYS results, considering that the higher-order shape functions of the eight-node ANSYS element should give it greater inherent accuracy (as well as greater computational cost).

10.3.2 Effect of Plate Thickness

A simply supported square plate example is used here to investigate the effect of plate thickness on the deflections and stresses. The plate has three layers with angles (0/90/0) and thicknesses of ($h/4$, $h/2$, $h/4$). Material properties of the laminae are $E_1/E_2 = 25$, $G_{12} = 0.5E_2$, $G_{13} = G_{23} = 0.2E_2$, and $\nu_{12} = 0.25$. Double sinusoidal loading was applied to the plate with a peak amplitude of q_0 at the centre. Again, one-quarter plate finite element models were used with the symmetry boundary conditions SS-1 (Table 3). Finite element results using Shell4 are presented for three meshes and three a/h ratios in Table 6, along with closed form solutions obtained with classical laminate theory (CLT), first-order shear deformation theory (FSDT) and exact results obtained with three-dimensional elasticity theory. Theoretical results reported here were obtained from a study by Reddy [33]. Table 7 gives the normalised quantities and locations where deflections and stresses were evaluated in both the Shell4 and the theoretical results.

Apart from the surprisingly large centre-plate deflections for $a/h = 10$, the Shell4 results generally compare well with the analytical results. The transverse shear stresses $\overline{\tau}_{xz}$ and $\overline{\tau}_{yz}$ predicted by Shell4 are in better agreement with the exact three-dimensional elasticity results than are those given by the FSDT. The reason for this is that the FSDT results in reference [33] were calculated using an isotropic shear correction factor $\kappa^2 = 5/6$, which is only a crude approximation for composite laminates. The extra work required to calculate shear correction factors by the method described in Section 2 therefore appears to be justified.

Variable	Analytical	Shell4			ANSYS		
	(Reddy)	2×2	4×4	8×8	2×2	4×4	8×8
Single Layer Orthotropic Plate (SS-1)							
$\overline{w}$	0.6497	0.6465	0.6466	0.6488	0.6636	0.6529	0.6505
$\overline{\sigma}_{xx}$	0.7866	0.6624	0.7611	0.7804	0.8527	0.8006	0.7900
$\overline{\sigma}_{yy}$	0.0244	0.0298	0.0251	0.0246	0.0241	0.0240	0.0243
$\overline{\tau}_{xy}$	0.0463	0.0270	0.0382	0.0435	0.0489	0.0481	0.0472
Cross-Ply (0/90) Plate (SS-1)							
$\overline{w}$	1.6955	1.6282	1.6805	1.6918	1.7033	1.6980	1.6961
$\overline{\sigma}_{xx}$	0.1268	0.1039	0.1211	0.1255	0.1376	0.1296	0.1275
$\overline{\sigma}_{yy}$	1.0761	0.8783	1.0278	1.0631	1.1671	1.0984	1.0818
$\overline{\tau}_{xy}$	0.0933	0.0657	0.0836	0.0902	0.1002	0.0960	0.0943
Angle-Ply (-45/45) Plate (SS-2)							
$\overline{w}$	1.0280	1.0091	1.0240	1.0278	1.0382	1.0313	1.0294
$\overline{\sigma}_{xx} = \overline{\sigma}_{yy}$	0.3504	0.2615	0.3238	0.3400	0.3679	0.3505	0.3466
$\overline{\tau}_{xy}$	0.4421	0.3534	0.4121	0.4370	0.4828	0.4631	0.4541
Angle-Ply $(-45/45)_4$ Plate (SS-2)							
$\overline{w}$	0.3858	0.3824	0.3847	0.3855	0.3959	0.3884	0.3864
$\overline{\sigma}_{xx} = \overline{\sigma}_{yy}$	0.2006	0.1511	0.1876	0.1970	0.2137	0.2030	0.2008
$\overline{\tau}_{xy}$	0.2637	0.2117	0.2449	0.2581	0.2854	0.2733	0.2679

Table 4: Results for four simply supported plate models.

Quantity	Location
$\overline{w} = w \times 100 E_2 h^3/qa^4$	$(a/2, a/2)$
$\overline{\sigma}_{xx} = \sigma_{xx}(h/a)^2/q$	G.P. nearest $(a/2, a/2)$ at $z = h/2$
$\overline{\sigma}_{yy} = \sigma_{yy}(h/a)^2/q$	G.P. nearest $(a/2, a/2)$ at $z = h/2$
$\overline{\tau}_{xy} = \tau_{xy}(h/a)^2/q$	G.P. nearest (a, a) at $z = -h/2$

Table 5: Normalized quantities and their evaluation points for thin plate results (G.P. = Gauss point).

a/h	Analysis	$\overline{w}$	$\overline{\sigma}_{xx}$	$\overline{\sigma}_{yy}$	$\overline{\tau}_{xy}$	$\overline{\tau}_{xz}$	$\overline{\tau}_{yz}$
10	3D Exact	7.434	0.599	0.403	0.028	0.301	0.196
	FSDT	6.627	0.496	0.359	0.024	0.414	0.128
	FE 2×2	9.259	0.420	0.323	0.021	0.248	0.138
	FE 4×4	8.582	0.476	0.359	0.024	0.271	0.148
	FE 8×8	8.418	0.490	0.368	0.024	0.276	0.150
20	3D Exact	5.173	0.543	0.308	0.023	0.328	0.156
	FSDT	4.491	0.524	0.294	0.022	0.434	0.108
	FE 2×2	5.755	0.446	0.261	0.019	0.262	0.114
	FE 4×4	5.454	0.504	0.292	0.022	0.285	0.124
	FE 8×8	5.379	0.519	0.300	0.022	0.291	0.126
100	3D Exact	4.385	0.539	0.271	0.021	0.339	0.139
	FSDT	4.337	0.535	0.269	0.021	0.442	0.100
	FE 2×2	4.588	0.459	0.231	0.018	0.269	0.103
	FE 4×4	4.415	0.518	0.261	0.021	0.291	0.112
	FE 8×8	4.370	0.533	0.269	0.021	0.297	0.115
CLT (Thin)		4.350	0.539	0.269	0.021	0.339	0.138

Table 6: Effect of thickness changes in a simply-supported, three-layer composite plate.

Quantity	Location
$\overline{w} = w \times 1000 E_2 h^3/q_0 a^4$	$(a/2, a/2)$
$\overline{\sigma}_{xx} = \sigma_{xx}(h/a)^2/q_0$	G.P. nearest $(a/2, a/2)$ at $z = h/2$
$\overline{\sigma}_{yy} = \sigma_{yy}(h/a)^2/q_0$	G.P. nearest $(a/2, a/2)$ at $z = h/4$
$\overline{\tau}_{xy} = \sigma_{xy}(h/a)^2/q_0$	G.P. nearest (a, a) at $z = -h/2$
$\overline{\tau}_{xz} = \sigma_{xz} h/a q_0$	G.P. nearest $(a, a/2)$, Layer 1
$\overline{\tau}_{yz} = \sigma_{yz} h/a q_0$	G.P. nearest $(a/2, a)$, Layer 2

Table 7: Normalized quantities and their evaluation points for thick plate results (G.P. = Gauss point).

11 Conclusions

A flat-facet quadrilateral shell element 'Shell4' has been developed for linear-elastic static analysis of laminated composite and non-composite applications in ship structures. This report has described the details of the element formulation and several examples have been presented comparing the performance of the element to comparable elements in VAST and ANSYS. The element has been shown to pass five patch tests, guaranteeing its convergence in all situations. Excellent performance was obtained for a number of examples of uniformly-loaded, simply supported composite plates examples. In shell and beam applications its performance is acceptable, but shows some slow convergence in problems with concentrated loading or warping. In these instances better accuracy would be obtained by using finer meshes, and hence a higher computational cost. No evidence of transverse shear locking or spurious modes has been observed in any of the examples tested to date. The element appears to be less sensitive to shape distortions in comparison to quadrilateral elements in ANSYS and VAST, as was shown in the cantilevered beam example of Section 10.2.1.

A better assessment of the performance will have to be obtained by testing on more realistic ship-structure related problems. Although the development and implementation of the Shell4 element has been generally successful, the author considers it advisable to conduct further research on element formulations before extending the element to dynamic and nonlinear ship-structure applications. Particularly important is assessing the applicability of the Shell4 element to nonlinear postbuckling analysis used in determining the ultimate strength of ship sections and components. It would also be useful to compare the performance of the Shell4 element with a four-node composite shell element based on the degenerate solid approach.

Acknowledgements

David Hally and David Heath provided helpful advice on C++ programming and their assistance is appreciated.

References

[1] *ANSYS Theory Reference Manual*, Ninth Edition (Release 5.5). Ed. Kohnke, P., ANSYS Inc., Canonsburg, PA., 1998.

[2] *Vibration and Strength Analysis Program (VAST): User's Manual*, Version #7.2. Martec Limited, Halifax, N. S., April 1997.

[3] *MAESTRO/Detailed Stress Analysis Graphics System: User's Manual.* Martec Limited, Halifax, N. S., May 1995.

[4] Heath, D., Pegg, N., Dinovitzer, A., and Walker, R., "Detail Analysis of Ship Structures", *Proceedings of the 5th Canadian Marine Hydrodynamics and Structures Conference*, St. John's, Newfoundland, July 1999.

[5] Zienkiewicz O. C., *The Finite Element Method*, Third Edition, McGraw-Hill, London, 1977.

[6] Cook, R. D., Malkus D. S., and Plesha, M. E., *Concepts and Applications of Finite Element Analysis*, Third Edition, Wiley, New York, 1989.

[7] Wilt, T. E., Saleeb, A. F., and Chang, T. Y., "A Mixed Element for Laminated Plates and Shells", *Computers and Structures*, Vol. 37, No. 4, pp. 597–611, 1990.

[8] To, C. W. S. and Wang, B., "Hybrid Strain-Based Three Node Flat Triangular Laminated Composite Shell Elements", *Finite Elements in Analysis and Design*, Vol. 28, pp. 177–207, 1998.

[9] Hughes, T. J. R., and Liu, W. K., "Nonlinear Finite Element Analysis of Shells: Part I. Three-Dimensional Shells", *Computer Methods in Applied Mechanics and Engineering*, Vol. 26, pp. 331–362, 1981.

[10] Oliver, J., and Oñate, E., "A Total Lagrangian Formulation for the Geometrically Nonlinear Analysis of Structures Using Finite Elements. Part I. Two-Dimensional Problems: Shell and Plate Structures", *International Journal for Numerical Methods in Engineering*, Vol. 20, pp. 2253–2281, 1984.

[11] Hinton, E. and Owen, R. J., *Finite Element Software for Plates and Shells*, Chapter 4, Pineridge Press, Swansea, 1984.

[12] Belytschko, T., and Wong, B. K., "Assumed Strain Stabilization Procedure for the 9-Node Lagrange Shell Element", *International Journal for Numerical Methods in Engineering*, Vol. 28, pp. 385–414, 1989.

[13] Kanoknukulchai, W., "A Simple and Efficient Finite Element for General Shell Analysis," *International Journal for Numerical Methods in Engineering*, Vol. 14, pp. 179–200, 1979.

[14] Dvorkin, E. N., and Bathe K. J., "A Continuum Mechanics Based Four-Node Shell Element for General Nonlinear Analysis", *Engineering Computation*, Vol. 1, pp. 77–88, 1984.

[15] Cook, R. D., "Four-Node 'Flat' Shell Element: Drilling Degrees of Freedom, Membrane-Bending Coupling, Warped Geometry, and Behaviour", *Computers and Structures*, Vol. 50, No. 4, pp. 549–555, 1994.

[16] MacNeal, R. H. and Harder, R. L., "A Refined Four-Noded Membrane Element with Rotational Degrees of Freedom", *Computers and Structures*, Vol. 28, No. 1, pp. 75–84, 1988.

[17] Hughes, T. J. R. and Tezduyar, T. E., "Finite Elements Based Upon Mindlin Plate Theory with Particlar Reference to the Four-Node Bilinear Isoparametric Element", *ASME Journal of Applied Mechanics*, Vol. 48, pp. 587–596, September 1981.

[18] Bathe K. J. and Dvorkin, E. N., "A Four-Node Plate Bending Element Based on Mindlin/Reisnner Plate Theory and a Mixed Interpolation", *International Journal for Numerical Methods in Engineering*, Vol. 21, pp. 367–383, 1985.

[19] Bathe K. J. and Dvorkin, E. N., "A Formulation of General Shell Elements—the Use of Mixed Interpolation of Tensorial Components", *International Journal for Numerical Methods in Engineering*, Vol. 22, pp. 697–722, 1986.

[20] Hughes, T. J. R., Taylor, R. L. and Kanoknukulchai, W., "A Simple and Efficient Element for Plate Bending", *International Journal for Numerical Methods in Engineering*, Vol. 11, pp. 1529–1543, 1977.

[21] Reddy, J. N., "On Refined Computational Models of Composite Laminates", *International Journal for Numerical Methods in Engineering*, Vol. 27, pp. 361–382, 1989.

[22] Reddy, J. N., "A Simple Higher-Order Theory for Laminated Composite Plates", *ASME Journal of Applied Mechanics*, Vol. 51, pp. 745–752, 1984.

[23] Reddy, J. N., "An Assessment of Four-Noded Plate Finite Elements Based on a Generalized Third-Order Theory", *International Journal for Numerical Methods in Engineering*, Vol. 33, pp. 1553–1572, 1992.

[24] Kant T., and Khare, R. K. "A Higher-Order Facet Quadrilateral Composite Shell Element", *International Journal for Numerical Methods in Engineering*, Vol. 40, pp. 4477–4499, 1997.

[25] Di Sciuva, M., "Evaluation of Some Multilayered Shear Deformable Plate Elements", *Computers and Structures*, Vol. 24, No. 6, pp. 845–854, 1986.

[26] Reddy, J. N., *Mechanics of Laminated Composite Plates - Theory and Analysis*. CRC Press, Boca Raton, 1997.

[27] Whitney, J. M., "Shear Correction Factors for Orthotropic Laminates Under Static Load", *ASME Journal of Applied Mechanics*, Vol. 40, pp. 302–304, March 1973.

[28] Whitney, J. M. and Pagano, N. J., "Shear Deformation in Heterogeneous Anisotropic Plates", *ASME Journal of Applied Mechanics*, Vol. 37, pp. 1031–1036, December 1970.

[29] Huang, H.-C., *Static and Dynamic Analyses of Plates and Shells*, Springer-Verlag, London, 1989.

[30] Naganarayana, B. P. and Prathap, G., "Force and Moment Corrections for the Warped Four-Node Quadrilateral Plane Shell Element", *Computers and Structures*, Vol. 33, No. 4, pp. 1107–1115, 1989.

[31] Irons, B., and Ahmad, S., *Techniques of Finite Elements*, Chap. 9, Ellis Horwood, Chichester, 1980.

[32] MacNeal R. H. and Harder, R. L., "A Proposed Standard Set of Problems to Test Finite Element Accuracy", *Finite Elements in Analysis and Design*, Vol. 1, pp. 3–20. 1985.

[33] Reddy, J.N., "Analysis of Layered Composite Plates Accounting for Large Deflections and Transverse Shear Strains", *Recent Advances in Non-Linear Computational Mechanics*, Ed. Hinton, E., Owen, D. R. J., and Taylor, C., Pineridge Press, Swansea, pp. 155–202, 1982.

UNCLASSIFIED
SECURITY CLASSIFICATION OF FORM
(highest classification of Title, Abstract, Keywords)

DOCUMENT CONTROL DATA

(Security classification of title, body of abstract and indexing annotation must be entered when the overall document is classified)

1 ORIGINATOR (the name and address of the organization preparing the document. Organizations for whom the document was prepared, e.g. Establishment sponsoring a contractor's report, or tasking agency, are entered in section 8.)

Defence Research Establishment Atlantic
PO Box 1012
Dartmouth, Nova Scotia, Canada B2Y 3Z7

2. SECURITY CLASSIFICATION (overall security classification of the document including special warning terms if applicable)

UNCLASSIFIED

3 TITLE (the complete document title as indicated on the title page. Its classification should be indicated by the appropriate abbreviation (S,C,R or U) in parentheses after the title)

A Flat-Facet Quadrilateral Element for Linear Elastic Analysis of Laminated Composite Plates and Shells

4 AUTHORS (Last name, first name, middle initial. If military, show rank, e.g. Doe, Maj John E.)

Malcolm J. Smith

5. DATE OF PUBLICATION (month and year of publication of document)	6a. NO. OF PAGES (total containing information. Include Annexes, Appendices, etc).	6b. NO. OF REFS (total cited in document)
January 2000	44	33

7 DESCRIPTIVE NOTES (the category of the document, e.g. technical report, technical note or memorandum. If appropriate, enter the type of report, e.g. interim, progress, summary, annual or final. Give the inclusive dates when a specific reporting period is covered).

TECHNICAL MEMORANDUM

8 SPONSORING ACTIVITY (the name of the department project office or laboratory sponsoring the research and development. Include address)

Defence Research Establishment Atlantic

9a. PROJECT OR GRANT NO (if appropriate, the applicable research and development project or grant number under which the document was written. Please specify whether project or grant).	9b. CONTRACT NO. (if appropriate, the applicable number under which the document was written).
Project 1.g.c.11	

10a ORIGINATOR'S DOCUMENT NUMBER (the official document number by which the document is identified by the originating activity. This number must be unique to this document.)	10b OTHER DOCUMENT NOs (Any other numbers which may be assigned this document either by the originator or by the sponsor.)
	DREA TM 1999-210

11 DOCUMENT AVAILABILITY (any limitations on further dissemination of the document, other than those imposed by security classification)

(X) Unlimited distribution
( ) Defence departments and defence contractors; further distribution only as approved
( ) Defence departments and Canadian defence contractors; further distribution only as approved
( ) Government departments and agencies; further distribution only as approved
( ) Defence departments; further distribution only as approved
( ) Other (please specify):

12. DOCUMENT ANNOUNCEMENT (any limitation to the bibliographic announcement of this document. This will normally correspond to the Document Availability (11). However, where further distribution (beyond the audience specified in (11) is possible, a wider announcement audience may be selected)

UNCLASSIFIED
SECURITY CLASSIFICATION OF FORM

13. ABSTRACT (a brief and factual summary of the document. It may also appear elsewhere in the body of the document itself. It is highly desirable that the abstract of classified documents be unclassified. Each paragraph of the abstract shall begin with an indication of the security classification of the information in the paragraph (unless the document itself is unclassified) represented as (S), (C), (R), or (U). It is not necessary to include here abstracts in both official languages unless the text is bilingual).

A flat-facet quadrilateral shell element 'Shell4' has been developed for linear-elastic static finite element (FE) analysis of laminated composite and non-composite applications in ship structures. The element formulation was developed by combining state-of-the-art formulations for quadrilateral plate bending and quadrilateral membrane elements with first-order shear deformation theory (FSDT) for laminates. The element is intended for use with general plate and shell configurations, involving isotropic, orthotropic, or composite material properties. In-plane rotations, also known as drilling degrees of freedom, have been included to permit correct element assembly in kinked or folded-plate type configurations, and special provision has been made for warped geometries. The element has been implemented in a finite element programme recently developed at DREA for linear static and first-ply failure analysis of composite structures. It is shown to pass all of the necessary patch tests to guarantee convergence. Validation is carried out using examples of isotropic beam and shell structures and composite plates taken from the finite element literature. The element is found to perform excellently for a number of problems involving a simply supported, uniformly-loaded composite plate. In shell and beam applications its performance is acceptable, although the element appears slow to converge at locations where concentrated loads are applied or in situations where elements are warped. The membrane response alone, however, appears to be quite good, and the element is less affected by mesh distortions than some other commercially available elements.

14. KEYWORDS, DESCRIPTORS or IDENTIFIERS (technically meaningful terms or short phrases that characterize a document and could be helpful in cataloguing the document. They should be selected so that no security classification is required. Identifiers, such as equipment model designation, trade name, military project code name, geographic location may also be included. If possible keywords should be selected from a published thesaurus, e.g. Thesaurus of Engineering and Scientific Terms (TEST) and that thesaurus-identified. If it not possible to select indexing terms which are Unclassified, the classification of each should be indicated as with the title).

Ship structure
Finite element analysis
Flat-facet
Quadrilateral shell element
Composite
Laminate
Fibre reinforced polymer

DCD03 2/06/87-M/ DREA mod 17 Dec 1997